



Contents lists available at ScienceDirect

Precambrian Research

journal homepage: www.elsevier.com/locate/precamres



Tectonic setting of the Balaram-Kui-Surpagla-Kengora granulites of the South Delhi Terrane of the Aravalli Mobile Belt, NW India and its implication on correlation with the East African Orogen in the Gondwana assembly

Yengkhom Kesorjit Singh^a, Bert De Waele^{b,c}, Subrata Karmakar^d,
Sunayana Sarkar^a, Tapas Kumar Biswal^{a,*}

^a Department of Earth Sciences, Indian Institute of Technology Bombay, Powai, Mumbai, Maharashtra 400076, India

^b SRK Consulting, 10 Richardson Street, West Perth, WA 6005, Australia

^c The University of Western Australia, 35 Stirling Highway, Crawley, WA 6009, Australia

^d Department of Geological Sciences, Jadavpur University, Kolkata 700 032, India

ARTICLE INFO

Article history:

Received 5 August 2009
Received in revised form 3 August 2010
Accepted 13 August 2010
Available online xxx

Keywords:

Aravalli Mobile Belt
South Delhi Terrane
Granulites
Zircon U–Pb SHRIMP dating
Neoproterozoic terrane
East African Orogen
Gondwana

ABSTRACT

Granulites are developed in various tectonic settings and during different geological periods, and have been used for continental correlation within supercontinent models. In this context the Balaram-Kui-Surpagla-Kengora granulites of the South Delhi Terrane of the Aravalli Mobile Belt of northwestern India are significant. The granulites occur as shear zone bounded lensoidal bodies within low-grade rocks of the South Delhi Terrane and comprise pelitic and calcareous granulites, a gabbro-norite-basic granulite suite and multiple phases of granites of the Ambaji suite. The granulites have undergone three major phases of folding and shearing. The F_1 and F_2 folds are coaxial along NE–SW axis, and F_3 folds are developed across the former along NW–SE axis. Thus, various types of interference patterns are produced. The granulite facies metamorphism is marked by a spinel–cordierite–garnet–sillimanite–quartz assemblage with melt phase and is synkinematic to the F_1 phase of folding. The peak thermobarometric condition is set at $\geq 850^\circ\text{C}$ and 5.5–6.8 kb. The granulites have been exhumed through thrusting along multiple ductile shear zones during syn- to post- F_2 folding. Late-stage shearing has produced cataclasites and pseudotachylites. Sensitive High Resolution Ion MicroProbe (SHRIMP) U–Pb dating of zircon from pelitic granulites and synkinematically emplaced granites indicate that: (1) the sedimentary succession of the South Delhi Terrane was deposited between 1240 and 860 Ma with detritus derived from magmatic sources with ages between 1620 and 1240 Ma; (2) folding and granulite metamorphism have taken place between ca. 860 and 800 Ma, and exhumation at around ca. 800–760 Ma; and (3) the last phase of granitic activity occurred at ca. 759 Ma. This shows, for the first time, that the granulites of the South Delhi Terrane are much younger than those of the Sandmata Granulite Complex of the northern part of the Aravalli Mobile Belt, the Saussar granulites of the Central India Mobile Belt and the Eastern Ghats Mobile Belt. Instead, they show similarities to the Neoproterozoic granulites of the Circum Indian Orogens that include the East African Orogen (East Africa and Madagascar), the Southern Granulite Terrane of India and much of Sri Lanka. We suggest that the South Delhi Basin probably marks a trace of the proto-Mozambique Ocean in NW India within Gondwana, that closed when the Marwar Craton, arc fragments (Bemarivo Belt in Madagascar and the Seychelles) and components of the Arabian-Nubian Shield collided with the Aravalli-Bundelkhand Protocontinent at ca. 850–750 Ma.

© 2010 Elsevier B.V. All rights reserved.

1. Introduction

Granulitic terranes play an important role in correlation across cratonic blocks within supercontinental assemblages. The tectonic

history of granulites, including deformation, metamorphism and exhumation, in conjunction with geochronology, has been used as criteria in such correlation studies. The granulites represent the lower crustal rocks and have been formed in various tectonic setting including compressional setting, as is the case for the Eastern Ghats Mobile Belt (Bhattacharya et al., 1994; Biswal et al., 2007) or the Saxonian Granulites (Franke, 1993), as well as in extensional setting (Weber, 1984) and subduction setting (Santosh et al., 2009b). Similarly, exhumation of the granulites has occurred

* Corresponding author. Tel.: +91 2225767280; fax: +91 2225767253.
E-mail addresses: bdewaele@srk.com.au (B. De Waele),
skarmakar@geology.jdvu.ac.in (S. Karmakar), tkbiswal@iitb.ac.in (T.K. Biswal).

through several processes including the overthrusting of nappes in a collisional orogen (Biswal and Sinha, 2003), decompression of the overlying crust, underplating by other crustal blocks, and oblique shearing along multiple retrograde shear zones in a transpressional setting (Sandiford and Powell, 1986). However, at the present level of exposure, granulites occur in two major forms, namely as extensive granulite terranes such as in the Napier Complex, Eastern Ghats Mobile Belt (Dasgupta, 1995; Mukherjee, 1998) and the Southern Granulite Belt (Hansen et al., 1984), and as shear bounded granulite lenses such as those in the Ivrea zone of the European Alps (Handy et al., 1999), Sandmata Granulite Complex of the Aravalli Mobile Belt (Guha and Bhattacharya, 1995; Dasgupta et al., 1997) and Saussar granulites in the Central India Mobile Belt (Bhowmik et al., 2005). The events of formation and exhumation may have been separated in time by several hundreds of millions of years, such as is the case for the Napier Complex (Harley, 1985), to only a few hundred million years as for the Hercynian granulites (Handy et al., 1999).

Indian granulites have been used for continental correlation studies between Antarctica, Australia and India in Gondwana assembly (Du Toit, 1937). In this paper we have studied a less known set of granulites on the Indian Peninsula, known as the Baram-Kui-Surpaga-Kengora granulites. These occur as a lensoidal body at the southwestern extremity of the South Delhi Terrane of the Aravalli Mobile Belt of northwest India (Fig. 1a). The results of this study are extremely significant in that the present-day configuration of crustal segments in the Indian cratonic assemblage, especially in view of ubiquitous presence of Neoproterozoic orogens, is considered to have largely resulted through Neoproterozoic amalgamation of Gondwana (Mezger and Cosca, 1999; Biswal et al., 2007; Collins et al., 2007a; Meert and Lieberman, 2008; Santosh et al., 2009b). Based on deformation patterns, metamorphism and uplift history, supported by zircon geochronology, the Baram-Kui-Surpaga-Kengora granulites show significant similarities with possible correlative terranes in the East African Orogen, with further implications on the Neoproterozoic assembly of Gondwana.

2. Regional geology

The NE-SW trending Aravalli Mobile Belt in western India is flanked by the Marwar and Mewar Cratons in the west and east, respectively (Fig. 1a and b). The Mewar Craton forms a promontory structure on the western edge of the Bundelkhand Protocontinent and the Aravalli Mobile Belt curves around it, forming a westerly closing flexure as a result of indentation tectonics, a process comparable to that which formed the Himalaya along the northern edge of the Indian Peninsula. The Mewar Craton is comprised of Mesoarchaean tonalite-trondhjemite-granodiorite (TTG) gneisses and sporadic greenstone belts (Mewar gneisses, 2.45–3.50 Ga, A-1 to A-5 in Fig. 1 and Table 1, Sivaraman and Odom, 1982; Macdougall et al., 1983; Gopalan et al., 1990; Wiedenbeck and Goswami, 1994; Roy and Kröner, 1996; Wiedenbeck et al., 1996a,b). However, the Marwar Craton is extensively intruded by the Erinpura and Malani granites, and in several places has been covered by younger volcano-sedimentary sequences belonging to the Sindreth, Puna-garh, and Marwar groups. Therefore, vestiges of the basement are only observed in restricted places (near Bar, Heron, 1953, Fig. 1). However, so far no Archaean isotopic age has been reported from Marwar Craton. The Aravalli Mobile Belt, which was visualised as a synclinorium by Heron (1953), has undergone major revisions and is now described to be a Proterozoic mobile belt consisting of a collage of NE-SW trending terranes juxtaposed along ductile shear zones, which have been shown as lineaments in the map (Fig. 1b). The terranes include the Aravalli, Hindoli-Jahajpur, Sandmata-

Mangalwar, Delhi and Sirohi terranes and comprise thick sequences of Proterozoic metasedimentary and meta-igneous rocks unconformably overlying the basement gneisses. The basal unconformity has been extremely tectonised and emplaced to various tectonic levels during Meso- and Neoproterozoic orogenesis.

The Aravalli Terrane is represented by low- to medium-grade rocks showing multiple phases of folding and granitic intrusions (Naha and Halyburton, 1974a,b; Naha and Mohanty, 1988; Roy, 1988; Sharma, 1988). Synkinematic granites provide a Palaeoproterozoic age for the terrane (ca. 2.0–1.8 Ga, P-1 and P-2 in Fig. 1 and Table 1, Choudhary et al., 1984; Wiedenbeck and Goswami, 1994). The Aravalli Terrane was an oceanic basin at 2.5 Ga, when sedimentation took place with shallow water stromatolite-bearing facies in the east and deep water carbonate-pelite facies in the west. The facies-domains have been separated by the ophiolite-bearing Rakhabdev shear zone that defines a subduction zone along which the Aravalli basin closed at 1.8 Ga (Deb et al., 1989; Sarkar et al., 1989; Sugden et al., 1990; Verma and Greiling, 1995).

The Hindoli-Jahajpur Terrane is considered by some to be part of the Aravalli Terrane based on lithological association, structure (Gupta, 1934; Heron, 1953; Bose and Sharma, 1992; Roy and Jakhar, 2002) and the Proterozoic age of the synsedimentary felsic volcanic rocks (1.8 Ga, P-3 in Fig. 1 and Table 1, Deb et al., 2001). However, other authors attribute it to the Archaean and suggest it forms part of the Bhilwara Supergroup, along with the Sandmata-Mangalwar Terrane (Raja Rao et al., 1971; Gupta et al., 1980; Sinha-Roy et al., 1998), while some regard it as an independent sequence of Palaeoproterozoic age (Porwal et al., 2006). The issue is far from being resolved.

The Sandmata- and Mangalwar Terranes are dominated by migmatitic gneisses (2.83 Ga, A-5 in Fig. 1 and Table 1, Tobisch et al., 1994), with sporadic enclaves of amphibolite and metapelite within it. Based on structural analysis, the gneisses have been explained to be the product of migmatitisation of the Aravalli rocks (Naha and Majumdar, 1971a,b; Naha and Halyburton, 1974a,b; Naha and Roy, 1983). The Sandmata Terrane occurs to the west and is marked by shear zone bounded granulite pockets known as the Sandmata Granulite Complex (Sharma, 1988; Deb et al., 1989; Guha and Bhattacharya, 1995; Dasgupta et al., 1997; Roy et al., 2005). The emplacement of these granulite pockets and granulite metamorphism in them are broadly synchronous, and date at ca. 1.7–1.8 Ga (P-5 in Fig. 1 and Table 1, Sarkar et al., 1989; Fareeduddin and Kröner, 1998). The above thermal event has reset the host rock Archaean migmatitic gneisses to younger ca. 1.8 Ga ages.

The Delhi Terrane, most extensive of all, is subdivided into the South- and North Delhi Terranes. The South Delhi Terrane occurs as a linear belt along the western edge of the Aravalli Mobile Belt. Internally the South Delhi Terrane has been subdivided into a number of longitudinal tectonic zones which are dominated by arenaceous facies in the east and calcareous facies in the west (Heron, 1953; Sen, 1981). Generally, the rocks of the South Delhi Terrane are marked by amphibolite facies metamorphism and multiple stages of folding. However, the terrane shows sporadic occurrence of granulite, tectonic slices of ophiolite, blue schist and basement gneiss (Desai et al., 1978; Naha et al., 1987; Biswal, 1988; Volpe and Macdougall, 1990; Tobisch et al., 1994; Biswal et al., 1998a,b; Fareeduddin and Kröner, 1998; Mukhopadhyay et al., 2000, 2010; Srikarni et al., 2004; Khan et al., 2005). Based on the ages of the synkinematic Sendra-Ambaji granite and diorite, the South Delhi orogeny is constrained between ca. 1.7 and 0.8 Ga (M-5, M-6 and M-7 in Fig. 1 and Table 1, Choudhary et al., 1984; Volpe and Macdougall, 1990; Tobisch et al., 1994; Deb and Thorpe, 2001; Deb et al., 2001; Pandit et al., 2003). The basin closed through subduction along the Kaliguman shear zone running along the contact between the Delhi and Aravalli Terranes (Sugden et al., 1990; Biswal et al., 1998a). However, a mineral (biotite) age of 535 ± 15 Ma has

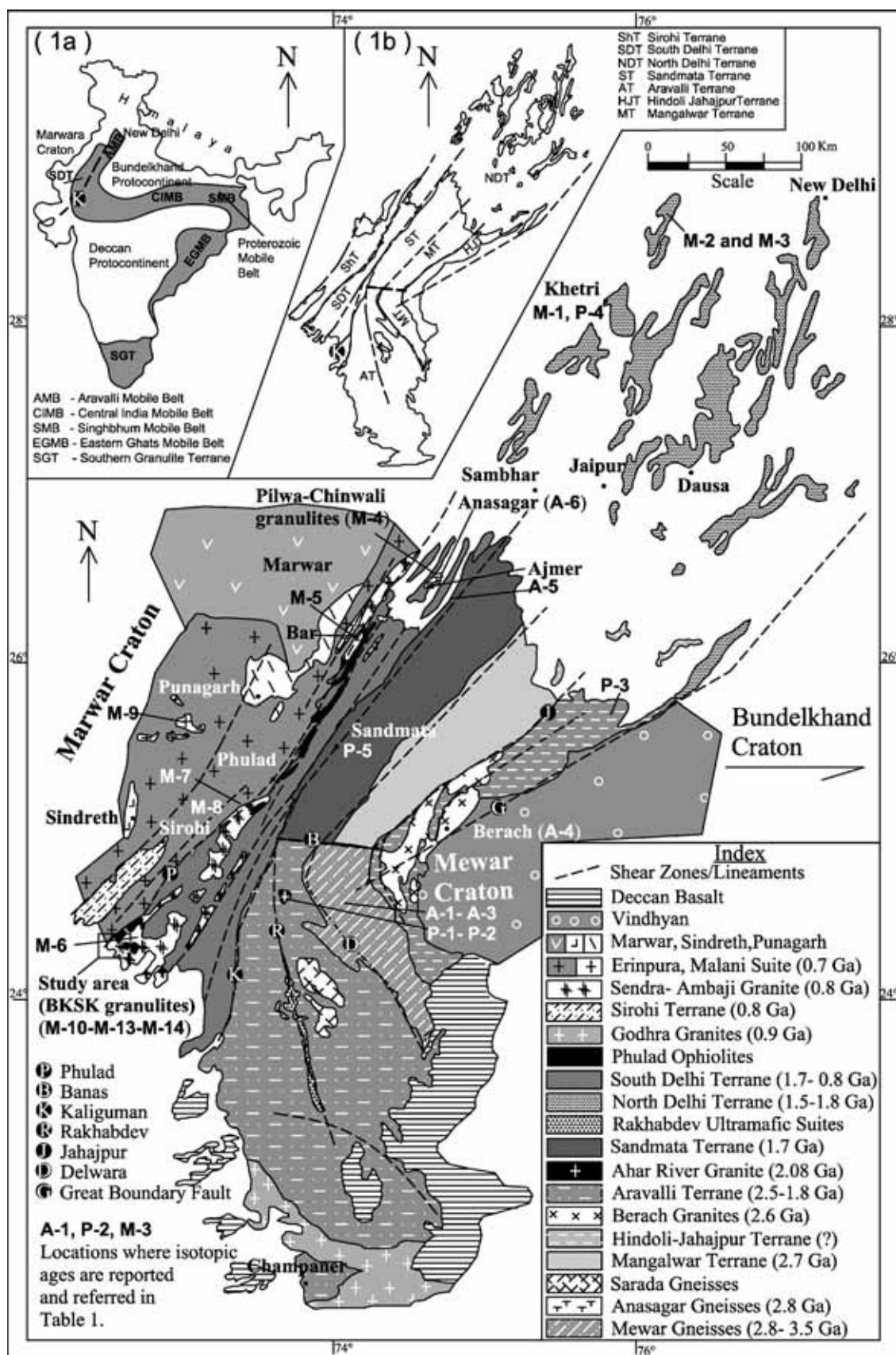


Fig. 1. Geological map of the Aravalli Mobile Belt, modified after Heron (1953), Gupta et al. (1980). Sandmata, Mangalwar, Hindoli-Jahajpur and Mewar gneisses were considered to be part of Bhilwara Supergroup. Inset shows the Proterozoic mobile belt (shaded in grey) that sutures the Bundelkhand- and the Deccan Protocontinent.

Table 1
Different formations in the Aravalli mobile belt, with their isotopic ages.

Location in Fig. 1	Formation	Age	Method	References
A-1	Mewar gneiss, amphibolites	2882 ± 46 Ma 3281 ± 3 Ma	Sm–Nd isochron age Zircon age	Gopalan et al. (1990) Wiedenbeck and Goswami (1994)
A-2	Untala granites	3500 Ma	Sm–Nd isochron	MacDougall et al. (1983)
A-3	Gingla granite	2620 ± 5 Ma 2505 ± 3 Ma	Single zircon evaporation Ion Microprobe Zircon	Roy and Kröner (1996) Wiedenbeck et al. (1996a,b)
A-4	Berach granite	2610 ± 50 Ma	U/Pb Zircon	Sivaraman and Odom (1982)
A-5	Country rocks of Sandmata Granulite Complex	2800 Ma	Sm–Nd isochron age	Tobisch et al. (1994)
A-6	Anasagar granite gneisses	2800 Ma 1849 ± 8 Ma	Sm–Nd Isochron age Single Zircon Evaporation	Tobisch et al. (1994) Mukhopadhyay et al. (2000)
P-1	Ahar River Granite	2026 ± 54 Ma	Rb–Sr isochron age	Wiedenbeck and Goswami (1994)
P-2	Amet Granite	1870 ± 200 Ma	Rb–Sr isochron age	Choudhary et al. (1984)
P-3	Felsic volcanic rocks, Hindoli-Jahajpur Terrane	1854 Ma	U–Pb Zircon age	Deb and Thorpe (2001)
P-4	Jasrapur granitoid, Khetri, North Delhi Terrane	1821.7 ± 0.4 Ma	Pb–Pb evaporation	Kaur et al. (2009)
P-5	Sandmata granulite	1725 + 14/–7 Ma 1723 + 14/–7 Ma	Single zircon evaporation age Single zircon evaporation age	Sarkar et al. (1989) Fareeduddin and Kröner (1998)
M-1	Bairat, Dadikar Granite; North Delhi Terrane	1600 Ma	Rb–Sr Whole Rock Isochron age	Gopalan et al. (1979) and Crawford (1970)
M-2	Rhyolite, Tosam	793 ± 18 Ma	Ar–Ar ages	Murao et al. (2000)
M-3	Granite, Tosam	818 ± 3.6 Ma	Ar–Ar ages	Murao et al. (2000)
M-4	Pelitic granulites, Pilwa–Chinwali	1434 ± 0.6 Ma	Single Zircon Evaporation	Fareeduddin and Kröner (1998)
M-5	Sendra Granite	840 Ma 967.8 ± 1.2 Ma	Rb–Sr age Pb/Pb ages	Choudhary et al. (1984) Pandit et al. (2003)
M-6	Granite gneisses, Ambaji	850 Ma	Rb–Sr age	Choudhary et al. (1984)
M-7	Diorites, South Delhi Terrane, Ranakpur	1012 ± 78 Ma	Sm–Nd Isochron age	Volpe and MacDougall (1990)
M-8	Erinpura granite	735 ± 15 Ma	Rb–Sr age	Crawford (1975)
M-9	Malani Igneous suite	771 Ma	U–Pb and 40Ar/39Ar	Meert and Lieberman (2008)
M-10	Rhyolite, South Delhi Terrane, Deri	987 ± 6 Ma	U–Pb zircon age	Deb et al. (2001)
M-11	Charnockite, BSKS granulites	757.8 ± 0.9 Ma	Single zircon age	Roy et al. (2005)
M-12	Microgranite	765 Ma	Rb–Sr age	Choudhary et al. (1984)
M-13	Folliated Granite, Siyawa	836 + 7/–5 Ma	U–Pb Zircon age	Deb et al. (2001)
M-14	Gabbar Hill granite near Ambaji	535 ± 15 Ma	Biotite mineral isochron age	Crawford (1975)
M-15	Sindreh volcanic rocks	765.9 ± 1.6 Ma	U–Pb Zircon age	Van Lente et al. (2009)

been reported from the sheared granites of the Ambaji area, marking a thermal disturbance (Crawford, 1975). Contrary to this, the North Delhi Terrane exhibits more extensive outcrops of quartzites and schists unconformably overlying the sialic basement rocks. The North Delhi Terrane is marked by late-stage open folding, axial planar shearing and low-grade metamorphism, and has been constrained to between 1.8 and 1.5 Ga (M-1, P-4 in Fig. 1 and Table 1, Crawford, 1970; Gopalan et al., 1979; Kaur et al., 2009).

The Sirohi Terrane occurs to the west of the South Delhi Terrane, and consists of low-grade metasedimentary rocks exhibiting multiple phases of deformation (Roy and Sharma, 1999). The terrane is extensively intruded by the Erinpura granites (ca. 850–735 Ma, M-8 in Fig. 1 and Table 1, Crawford, 1975; Choudhary et al., 1984), the Malani igneous suite (ca. 793–818 Ma, M-9 in Fig. 1 and Table 1, Bhushan, 2000; Murao et al., 2000; 827.0 ± 8.8 Ma, Pradhan et al., 2010) and Sindreh volcanics (765.9 ± 1.6 Ma, M-15, Van Lente et al., 2009).

3. The study area

The Baram–Kui–Surpagla–Kengora granulites (hereafter will be referred as BSKS granulites) occur as a lensoidal body on the southern tip of the South Delhi Terrane, and are marked by several shear zones; the Surpagla shear zone defines the eastern margin with the low-grade rocks of the Ambaji basin, the Kui–Chitraseni shear zone marks the western margin and the Ghoda-, Jogdadi-, Baram shear zones occur within the terrane (Figs. 2 and 3).

3.1. Rock types

The BSKS granulites comprise pelitic and calcareous metasedimentary granulites; a gabbro–norite–basic granulite suite, and several phases of felsic granitoid rocks called the Ambaji granites (Figs. 4–6). The pelitic granulites exhibit prominent migmatitic structures (Fig. 4a). The paleosomes contain spinel, sillimanite,

cordierite, garnet, biotite and zircon with rare kyanite, andalusite and sapphirine. Cordierites are elongated and carry inclusions of spinel and sillimanite (Fig. 6a). Calcareous granulites show the presence of diopside, anorthositic plagioclase, wollastonite, scapolite and zoisite forming resistant layers. Garnet is rare and diopside carries inclusions of plagioclase and relict hornblende (Fig. 4b). Diopside–wollastonite–vesuvianite skarns are developed in the calcareous granulites at the contact with the gabbro–norite–basic granulite pluton as well as granitic intrusives. The pelitic and calcareous granulites are interlayered with metarhyolites and metabasalts, representing rift-related synsedimentary lava flows in the basin. The metabasalts have been converted to amphibolites, and in places highly flattened pillow structures have been recognised. The metarhyolites appear as microgranites with hornblende and occasional hypersthene. In an earlier study Biswal et al. (1998b) suggested that the Delhi sediments were deposited in a passive continental margin.

The gabbro–norite–basic granulite plutons are of gabbro–norite composition at the core without any sign of metamorphism, while towards the periphery the plutons show metamorphism to basic granulites with orthopyroxene, clinopyroxene, hornblende and plagioclase. Metamorphic foliation is defined by the growth of tabular hornblende and hypersthene parallel to S_1 fabric. The gabbro–norite members of the pluton carry magmatic layering developed due to mineral segregation. The layers range in thickness from a few mm to a meter, and vary widely in composition from anorthosite, troctolite to pyroxenite (Fig. 4c). Biswal et al. (1998a) reported a calc–alkaline affinity of the gabbro–norite–basic granulite suite and interpreted the suite to have been emplaced in a magmatic arc setting. More recently, Khan et al. (2005) interpreted the mafic and ultramafic units to form part of an ophiolite. However, none of these rocks shows oceanic signatures.

The Ambaji Granites have been identified to consist of three phases. The G1 phase is closely associated with pelitic granulites, carries undigested paleosome patches bearing spinel, cordierite

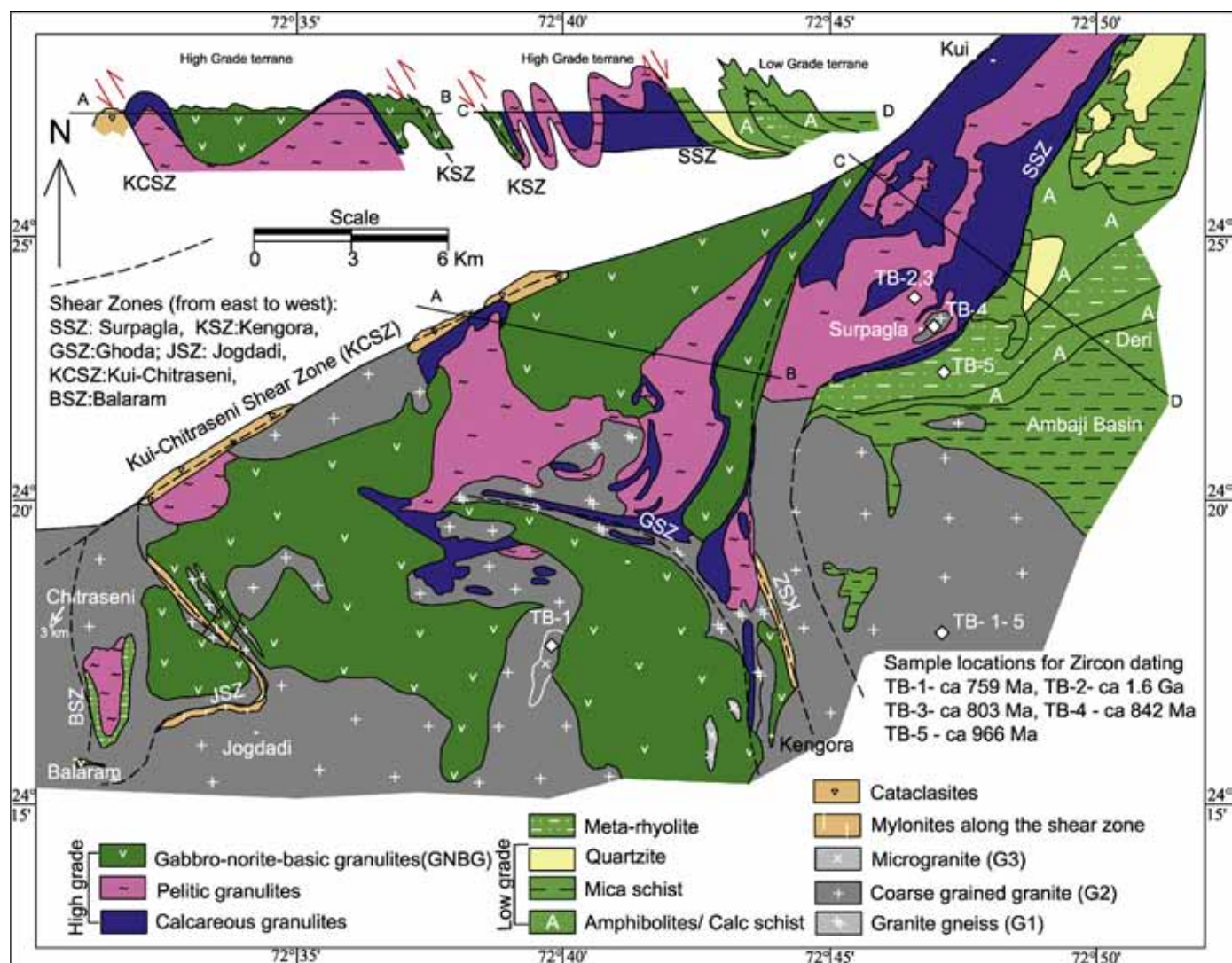


Fig. 2. Lithological map of the study area. To the top left, Section along AB shows the granulite blocks marked on either side by northwesterly verging thrusts (Kui-Chitraseni and Kengora shear zone) which are responsible for exhumation of the high-grade rocks to the present level. CD section shows Surpagla shear zone to be a normal slip fault; the high-grade terrane in the west has been uplifted with respect to low-grade terrane.

and sillimanite and shows similar deformational structures as migmatites. Thus it is interpreted that the G1 phase has been produced from the melting of the pelitic rocks during synkinematic F₁ folding and high-grade metamorphism. The G2 phase is very coarse-grained, with quartz, alkali feldspar and biotite, and rare garnet, muscovite and zircon. The granites occur as batholiths, intruding into the metasedimentary rocks along the axial planes of F₂ folds, and shear zones producing extensive metasomatic alteration in country rock. The G3 phase is synkinematic to F₃ folding and it is generally medium grained and occurs as dykes, veins or lensoidal bodies.

In contrast to these high-grade rocks, the low-grade rocks in the Ambaji basin consist of mica schist, quartzite, calcareous schist, pillow-bearing metabasalt and metarhyolite. These are intruded by amphibolites dykes and G2 and G3 phases of granites.

3.2. Structure

The BKS granites have undergone three major phases of folding. The first two phases, namely F₁ and F₂, are coaxial, and have developed Type 3 interference patterns from mesoscopic to map scale (Fig. 4a and b). A progressive deformation ensuing from NW-

SE shortening of the basin has been attributed to such coaxial deformation. The F₁ folds are developed on the bedding surfaces in form of isoclinal, extremely drawn out and flattened parallel folds, with development of marked penetrative axial planar fabric S₁. The S₁ is represented by migmatitic banding in the pelitic granulites and gneissosity in the calcareous granulites. Shape preferred orientation of sillimanite, spinel, biotite, cordierite and garnet in the pelitic granulites, and plagioclase, calcite and diopside in the calcareous granulites and orthopyroxene, clinopyroxene, hornblende and plagioclase in basic granulites define such fabric. This further suggests that crystallisation of the above minerals marking the granulite facies metamorphism is synkinematic to F₁ folding. Further, melting of the rocks during F₁ folding has produced the migmatites, and the G1 phase of granites. Emplacement of the gabbro-norite-basic granulite plutons has happened synkinematically with F₁ folding. This is evident from the F₁ folding of the magmatic banding in the pluton, boudinage formation due to synkinematic flattening of the gabbro-norite-basic granulite veins emplaced along S₁ planes, and granulite facies metamorphism of the pluton-margins and the associated veins.

The F₂ folds are open and upright and form crenulation cleavages, discrete axial planar shear fractures and shear bands along

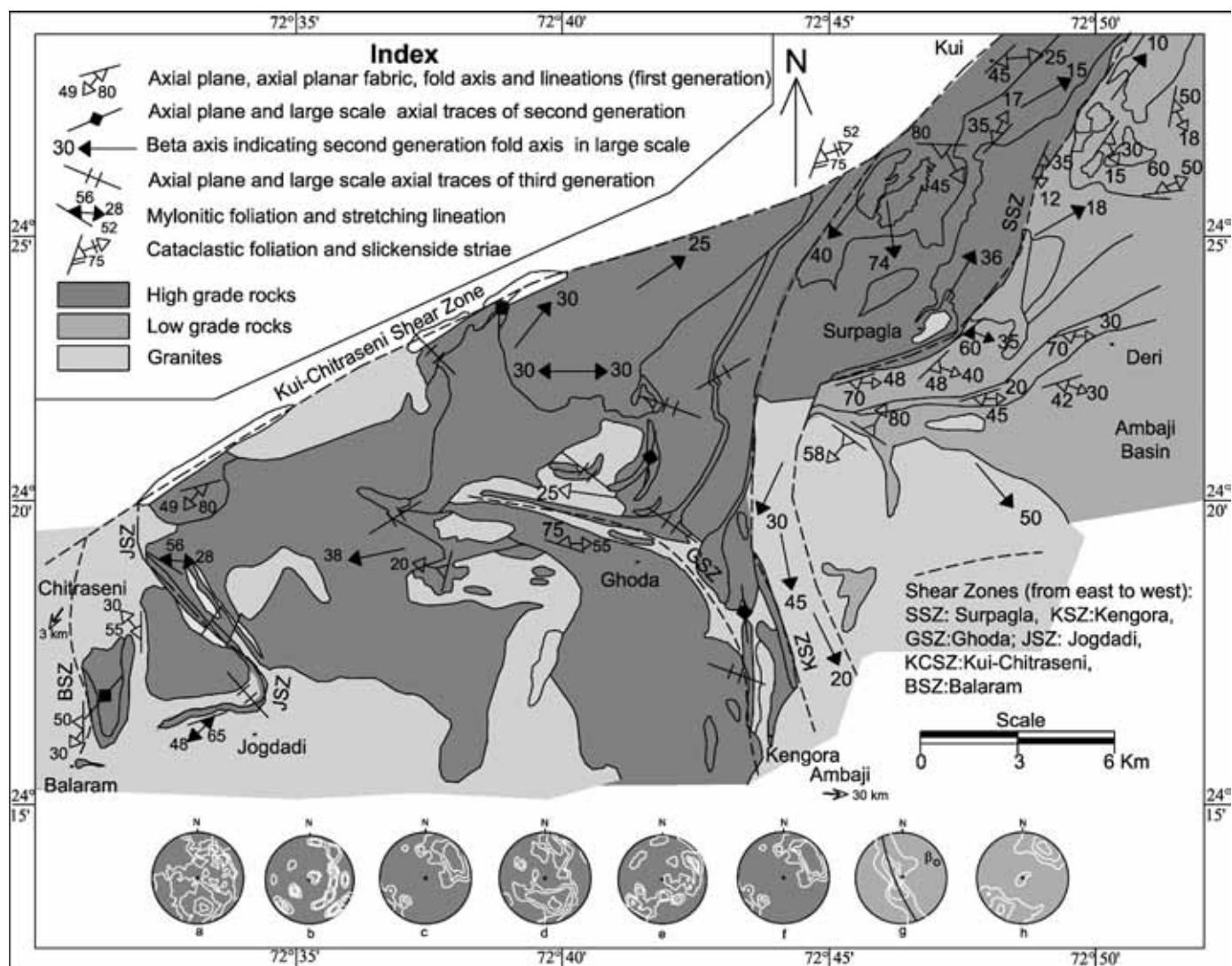


Fig. 3. Structural map of the study area. Stereograms (a)–(h) show analysis of structural fabrics collected from entire area. (a–f = high-grade rocks, g and h = low-grade rocks). (a) 350 F_1 fold axes and lineations of SW part; contour: 1, 3, 7%. (b) 300 F_1 fold axes and lineation of central part; contours: 1, 3, 7%. (c) 140 F_1 fold axes and lineation of NE part; contours: 1, 3, 7%. (d) 92 F_2 fold axes and lineation of SE part; contours: 1, 3, 7%. (e) 75 F_2 fold axes and lineation of central part; contours: 1, 3, 7%; (f) 50 F_2 fold axes and lineation of NE part; contours: 1, 3, 7%. (g) 130 s_1 planes and beta axes for low-grade area Ambaji basin; contours: 1, 3, 5%. (h) 150 f_1 – f_2 fold axes and lineation of low-grade rocks; contours: 1, 3, 5%.

the limbs (Fig. 4d and e). From the study of the mylonites and buckle folds within such shear bands, and mapping of the large-scale shear zones, it has been interpreted that the large-scale ductile shear zones, namely the Kui-Chitraseni-shear zone, Surpaga-, Kengora-, Jogdadi- and Balaram shear zone have been developed during F_2 folding (Figs. 2 and 3). The shear zones are found axial parallel to the large-scale F_2 folds (Fig. 3). Upper amphibolite facies metamorphism has occurred during F_2 folding. This is evident from the growth of fibrous sillimanite and biotite along the axial plane of the F_2 fold (Fig. 6d), garnet and cordierite at the hinge zone, and kyanite along the shear bands. However, melting of the metasediments is not evident. G2 granites have been emplaced during this stage of folding, invoking extensive feldspathisation along the shear bands in the basic granulites.

F_3 folds are developed in form of warps, kinks and chevron folds in a polyclinal fashion along NW-SE and ENE-WSW direction. This has produced Type 1 and Type 2 interference patterns on superposition over F_1 and F_2 folds, respectively (Fig. 5a and b). From the analysis of the conjugate kinks in the study area and elsewhere (Naha et al., 1984), compression direction during F_3 folding

is deduced to be NE-SW. The F_3 folding has taken place at shallower level of the crust as indicated by low-grade metamorphic minerals like biotite and phlogopite, crystallised parallel to the axial plane of the folds. Microgranite veins (G3) have been emplaced along the F_3 shear fractures.

The large-scale structure of the area is mainly controlled by NW-SE trending F_3 folds (Fig. 3). The lithounits as well as the shear zones, which were initially NE-SW due to the effect of F_2 folding, swerve from NE-SW to E-W and NW-SE, and the F_1 – F_2 fold axes show variation from sector to sector (Fig. 3 stereoplots). This variation is further augmented due to larger concentration of gabbro-norite-basic granulite plutons in the SW. The ductile shear zones are other large-scale structures in the area. They vary in width from a few meters to hundreds of meters and run for kilometers over several rock types, thus the mylonitic composition varies from place to place. Mylonitic fabrics suggest thrust slip character, implying that the granulite terrane has been exhumed through thrusting (Fig. 4f). However, the easternmost shear zones shows normal slip with respect to the low-grade terrane. As the F_3 folding has happened subsequent to thrusting, shear zones in several parts are overprinted by low-grade metamorphism. Further, some

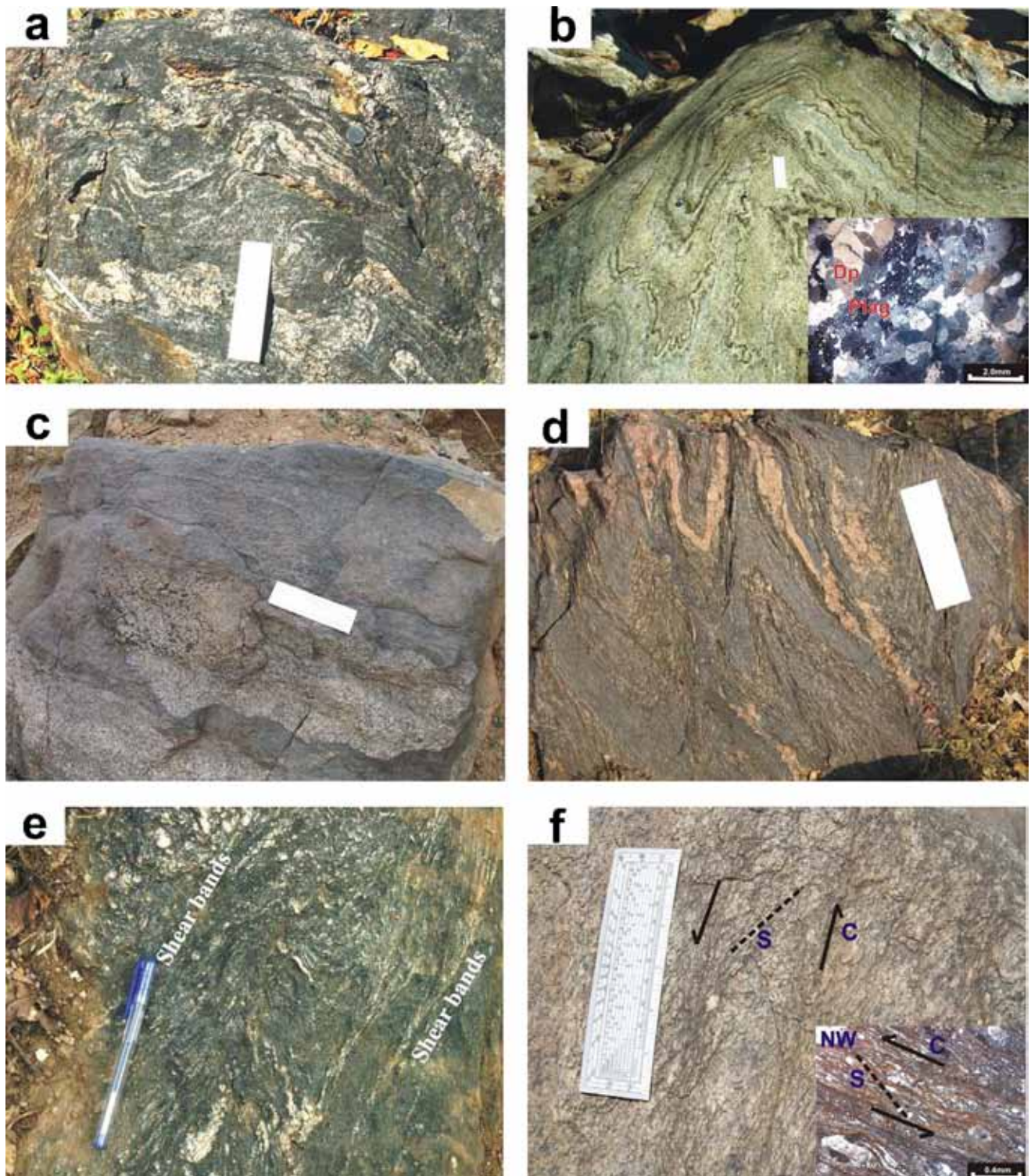


Fig. 4. (a) Pelitic granulites showing migmatitic structure; alternate paleosome and neosome define the S_1 fabric in the rock. Due to synkinematic nature of migmatization with F_1 folding, migmatitic layers, at places, are folded by F_1 folds which are isoclinal and recumbent (coin is at the F_1 hinge). F_2 fold (scale is kept parallel to the F_2 axial plane) has been superimposed on F_1 to produce Type 3 interference pattern. (b) Calcareous granulites showing ribbed structure due to differential weathering of carbonate layers (white) with respect to silicate layers (dark). These layers define the bedding which have been folded coaxially by F_1 (marked by coin at the hinge) and F_2 fold (scale parallel). Inset shows minerals (Dp–diopside and Plag–plagioclase) present in the rock. (c) Gabbro–norite members of the gabbro–norite–basic granulite suite show segregation of plagioclase. The suite shows a variation in composition, the parts occurring close to the host pelitic and calcareous granulites have been metamorphosed to basic granulites while those occur in the core show gabbro, norite and at places anorthositic composition. (d) F_2 crenulation in pelitic granulites, developed on S_1 fabric. Discrete shear fractures are developed parallel to S_2 cleavage (scale parallel). (e) Shear bands are developed along the limb of the F_2 fold. Mylonitisation has occurred along the shear bands and folds are developed due to shortening across the zone. These folds are similar with F_2 folds. (f) S–C fabric in the granite mylonites from the Ghoda Shear Zone (GSZ – Figs. 2 and 3). The photograph is to be rotated 70 degrees anticlockwise to get the perspective of thrust slip sense of shear. The S–C fabric observed under thin section (inset) confirms NW vergence of the thrust. (For interpretation of the references to color in this figure legend, the reader is referred to the web version of the article.)

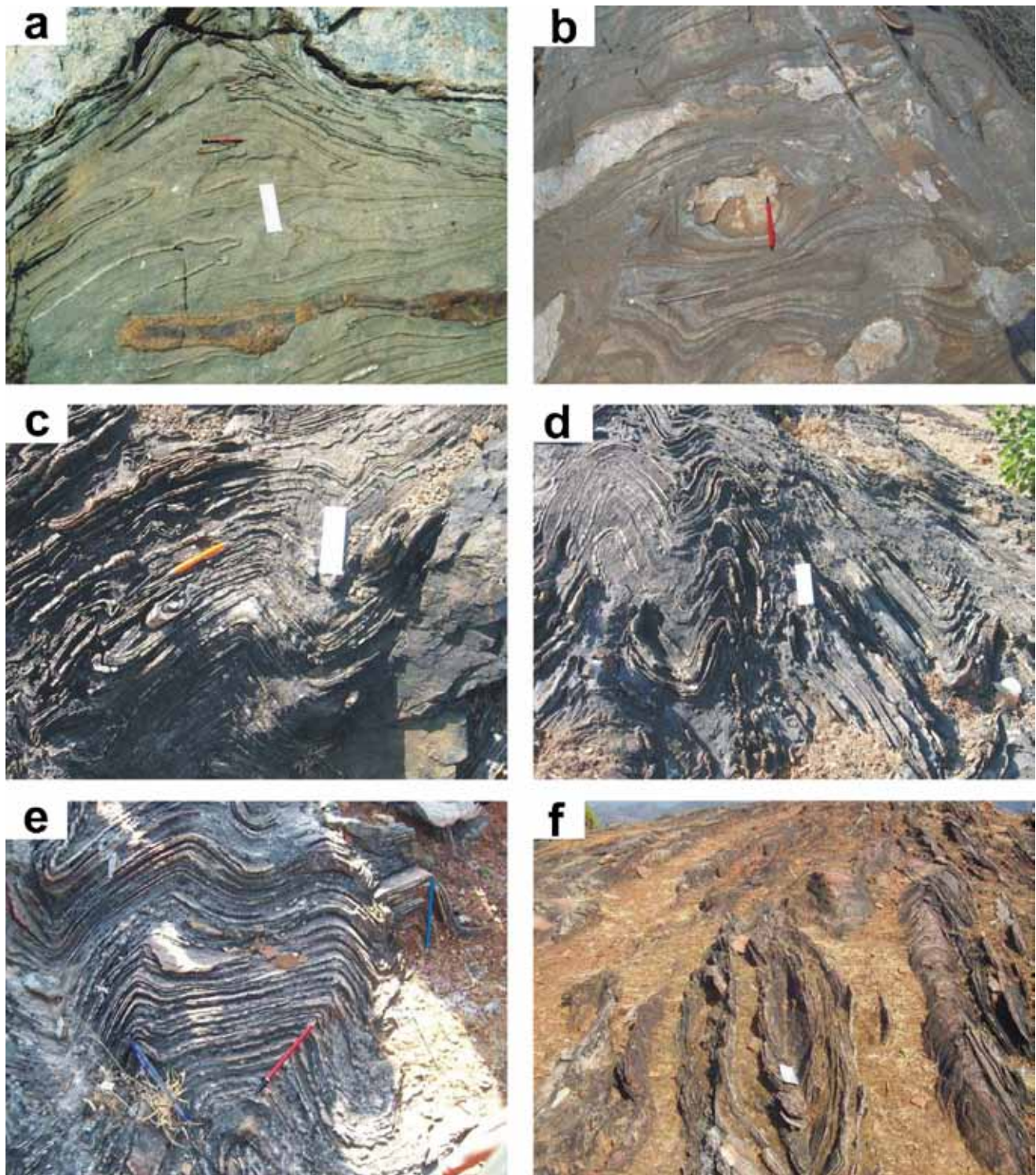


Fig. 5. (a) Mirror image pattern in the calc granulites, this is developed due to superposition of F_3 (scale parallel) on the reclined F_1 folds (pencil parallel). (b) Dome and basin structures in the calcareous granulites, produced from the superimposition of F_3 fold (red pen) on F_2 folds (white pencil). G2 Granites are emplaced in the core of the F_2 fold. (c) Type 3 interference pattern in calcareous schists of the low-grade terrane, produced from the coaxial folding between isoclinal and reclined – f_1 fold (pencil parallel) with open and upright – f_2 fold (scale parallel). (d) Axial plane parallel shearing in the f_2 fold; large-scale shear zones are, however, not observed in the low-grade terrane. (e) Conjugate f_3 folds (axial plane marked by pen and pencil) in closely foliated calcareous schist of the low-grade terrane, the orientation of the obtuse angle bisector of the conjugate indicates horizontal compression in NNE–SSW direction. (f) Dome and basin structures developed due to interference of f_2 and f_3 folds in the calcareous schist of the low-grade terrane. (For interpretation of the references to color in this figure legend, the reader is referred to the web version of the article.)

of the shear zones, e.g. the Kui–Chitraseni shear zone, have been reactivated later as brittle faults hosting cataclasites and pseudotachylites (Biswal et al., 2004; Sarkar and Biswal, 2005; Anbazhagan et al., 2006).

The Ambaji basin shares a common deformational history as the BKS granulates, consisting of an early phase of coaxial folding between f_1 and f_2 folds along NE–SW axis (Fig. 5c and d) followed by f_3 folds (Fig. 5e) along NW–SE axis (lowercase font is used to

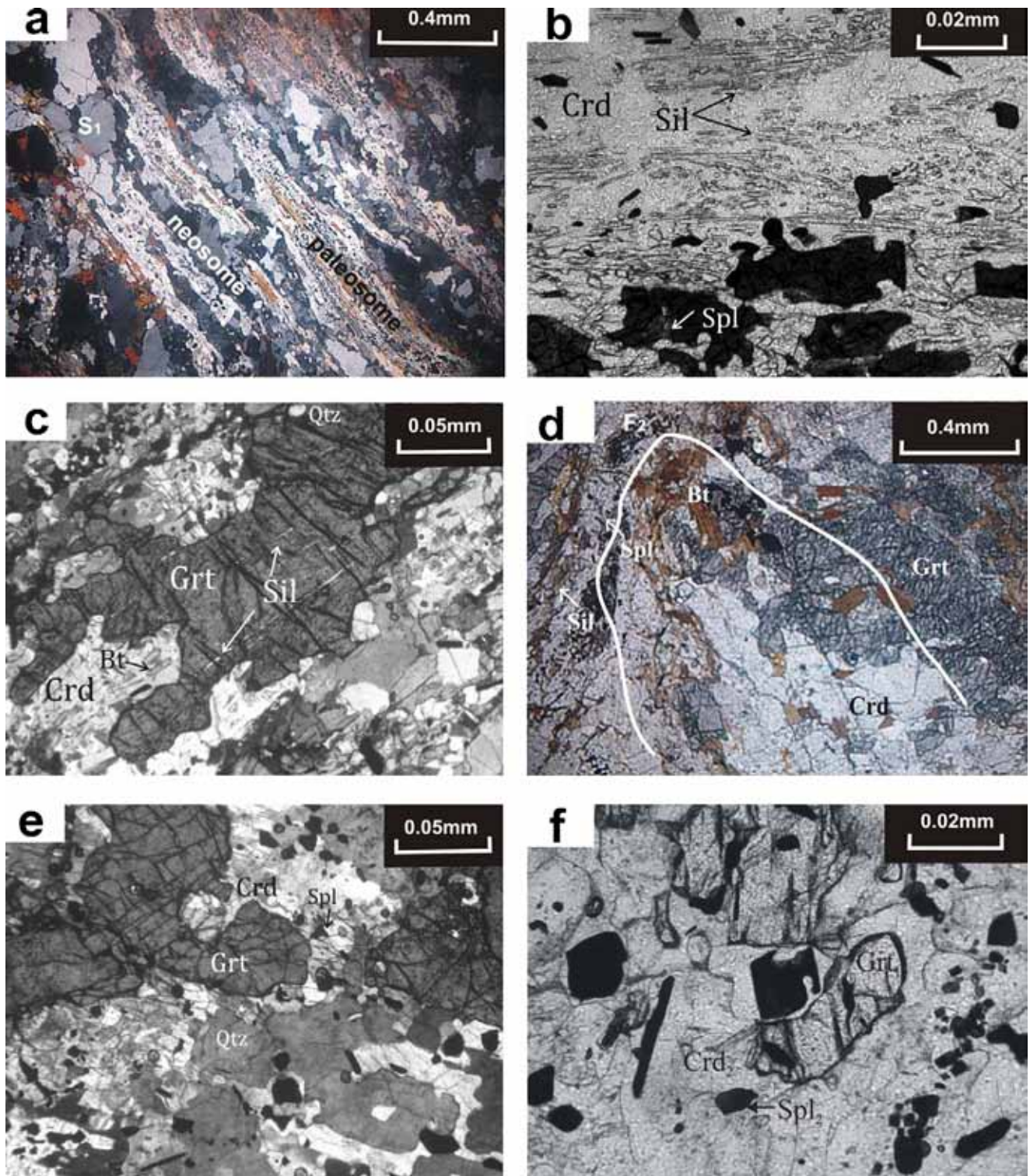


Fig. 6. (a) Photomicrograph of pelitic granulites showing S_1 fabric. The neosome is defined by quartzofeldspathic layers and the paleosome is defined by the cordierite–sillimanite–spinel layers. (b) Detailed photomicrograph of paleosome, showing cordierite ($Cr d_1$) porphyroblasts with internal schistosity defined by sillimanite (Sil) inclusions. Note the presence of spinel (Spl) at the contact with cordierite. These belong to S_{il1} and S_{pl1} . (c) Photomicrograph of pelitic granulites, showing garnet porphyroblasts with sillimanite (Sil) and quartz (Qtz) inclusions. Associated cordierite (Crd) contains inclusions of biotite (Bt). All these minerals belong to F_1 stage. (d) F_2 fold show synkinematic growth of biotite, garnet, sillimanite and spinel parallel to the axial plane of the fold. This assemblage reflects a retrograde phase that happened subsequent to the exhumation of the granulites. (e) Garnet (Grt) is surrounded by cordierite (Crd) and spinel (Spl) against quartz (Qtz) grains in pelitic granulites. These are $Cr d_2$ and S_{pl2} . These belong to retrograde phase. (f) Photomicrograph of pelitic granulites, cordierite₂ develops only around Grt_1 or S_{pl1} against quartz. (For interpretation of the references to color in this figure legend, the reader is referred to the web version of the article.)

designate folds in low-grade units). The superposition of folds has produced Type 1, 2 and 3 interference patterns (Fig. 5c and f). A discrete axial planar fracture cleavage S_2 , showing refraction across layers of different competence, pervades the rocks. Some of these fractures show meter-scale shear displacement (Fig. 5d), but large-scale ductile shear zones are not observed. The Ambaji basin represents a large-scale southwesterly plunging F_2 fold which has a NE–SW axial plane, overturned to the NW. As a result, both limbs show a southeasterly dip. This is further indicated by girdle distribution of the S_1 schistosity planes (Fig. 3g).

Cross-sections A–B and C–D (Fig. 2 inset) indicate that the rock units are folded by large-scale F_2 fold. The folded GNBG plutons have been pinched out within the metasediments due to its synkinematic nature of intrusion during F_1 . The high-grade terrane has been exhumed through thrusting along the terrane margin shear zones namely Kui–Chitraseni shear zone and Surpagla shear zone and internal shear zones (Fig. 2 inset). This has placed granulites against the low-grade rocks of the Ambaji basin. Therefore, the Kui–Chitraseni shear zone that marks the western margin show NW vergence thrust slip while the eastern margin shear zone, the Surpagla shear zone, shows normal slip to the SE.

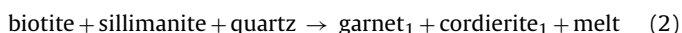
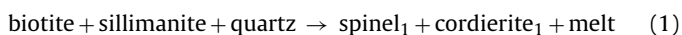
3.3. Metamorphism in the BKS granulates

3.3.1. Petrology of the pelitic granulites

The pelitic granulites have been studied to determine the physico-chemical condition of metamorphism of the rocks. A lower pressure metamorphism was qualitatively suggested by Desai et al. (1978) based on the presence of cordierite in the pelitic granulites. The rocks are characterized by compositional banding, with darker layers alternating with quartzofeldspathic leucosomes. The dark layers show concentration of spinel, cordierite, garnet and sillimanite. These minerals crystallized during F_1 folding. Hence a prograde stage during the F_1 folding is envisaged.

3.3.1.1. Prograde stage and the peak metamorphic assemblages.

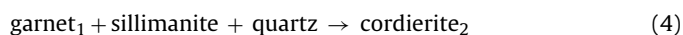
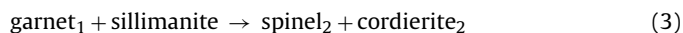
Cordierite (Cr_{d1}) occurs as flattened porphyroblasts containing numerous inclusions of sillimanite (Fig. 6a and b) whereas a porphyroblastic variety of garnet (Grt_1) preserves rare inclusions of biotite, sillimanite and quartz, which define an internal schistosity (Fig. 6c). Spinel (Spl_1) occurs in the matrix as medium-sized grains that are intergrown with Cr_{d1} . The sillimanite–biotite–quartz inclusions in Cr_{d1} and Grt_1 , defining the early schistosity, are interpreted to form part of the assemblage stabilised during the prograde stage of evolution. Subsequently, this mineral assemblage gave rise to Cr_{d1} , Grt_1 and Spl_1 . Presence of quartzofeldspathic leucosomes suggest former occurrence of melt. We therefore interpret the stabilisation of Grt_1 , Cr_{d1} and Spl_1 due to dehydration-melting of a protolith containing biotite–sillimanite–quartz (Grant, 1985a,b; Vielzeuf and Holloway, 1988; Le Breton and Thompson, 1988; Waters, 1988, 1991) via the model reactions:



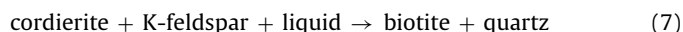
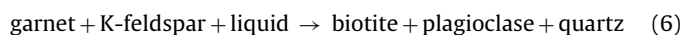
The reactions (1) and (2) may take place simultaneously in micro domains and may be controlled by variations in bulk chemistry. Fe_3O_4 rich spinel suggests that the melting event probably took place under high fO_2 conditions.

3.3.1.2. Retrograde stage. The F_2 folding is marked by growth of finer cordierite, sillimanite, spinel and biotite (Fig. 6d) that indicates a retrograde origin. This has happened subsequent to the exhumation of the granulites to the higher level. Porphyroblastic garnet is surrounded by a symplectite of finer grained cordierite (Cr_{d2}) and spinel (Spl_2) (Fig. 6e) and, in rare instances, small to medium-sized skeletal garnet grains show a cordierite₂ corona around them.

Sometimes cordierite₂ develops only around Grt_1 or Spl_1 against quartz (Fig. 6f). The following FMAS model reactions can be predicted to account for the evolution of the second generation of cordierite and spinel during retrogression:



The occurrence of coarse matrix biotite in contact with garnet and cordierite suggest the late hydration reactions to develop this retrograde phase to be:



3.3.2. Mineral chemistry, electron microprobe analysis

Mineral chemistry of the coexisting phases in the pelitic granulites was determined by JEOL-JXA-8600 M WDS based electron microprobe at Indian Institute of Technology, Roorkee. The operating conditions were 15 kV accelerating voltage, 20 nA specimen current 2 μm beam diameter. Both synthetic and natural mineral standards were used for calibration, with ZAF correction applied. (The analytical result has been stored as Table 3 in the Journal web site.)

Garnet₁ is essentially almandine rich ($X_{Alm} \sim 0.8$) with very low amounts of pyrope (maximum $X_{Prp} = 0.13$) and insignificant grossular and spessartine component. Cordierite is characteristically enriched in Fe^{2+} where X_{Mg} varies from 0.44 to 0.58. There is no compositional distinction between two generations of cordierite. Spinel₁ is hercynitic ($X_{Hc} = 0.70–0.77$) in composition and is characteristically enriched in ZnO ($X_{Gah} = 0.08–0.21$) and low in Cr_2O_3 . Recalculated Fe_2O_3 contents in spinel range from 3.52 to 5.88. Biotite is moderately rich in TiO_2 (3.5–4.2) and poor in phlogopite component ($X_{Mg} = 0.31–0.41$).

3.3.3. P–T condition of metamorphism

Peak pressure and temperature conditions of metamorphism were deduced using conventional thermobarometers applicable to the peak metamorphic assemblage. Maximum temperatures, estimated using the garnet–cordierite thermometer of Bhattacharya et al. (1988) are $\sim 700^\circ\text{C}$ at an estimated pressure of 6 kb. The spinel–quartz–cordierite geothermometer of Nichols et al. (1992) gave a similar value. A higher temperature ($\leq 900^\circ\text{C}$) was estimated using the spinel cordierite thermometer of Vielzeuf (1983). Garnet–cordierite–aluminosilicate–quartz and garnet–spinel–aluminosilicate–quartz barometry record pressures of 5.3–6.8 kb at estimated temperature of 800°C , whereas the garnet–cordierite and spinel–quartz–cordierite barometer (Nichols et al., 1992) gave slightly lower estimates. We estimate peak temperature and pressure of $\geq 850^\circ\text{C}$ and 5.5–6.8 kb for the studied rock.

A P–T pseudosection constructed by Kelsey (2008) for bulk rock $X_{Mg} = 62$ constrains the P–T domain for the peak assemblage of garnet–cordierite–spinel–K-feldspar with liquid at ≤ 7.5 kb and 925°C . The stability range of this assemblage is consistent with the experimental data of similar bulk rock composition at high fO_2 condition (Das et al., 2003) and with the semi-quantitative petrogenetic grid of Dasgupta et al. (1995) in the system KFMASH. That garnet–cordierite–spinel–sillimanite is a relatively low pressure assemblage is also supported by the qualitative KFMASH grid of McDade and Harley (2001). Stabilisation of spinel and quartz is well known in several HT/UHT metamorphic terrains (e.g. Lal et al., 1987; Sandiford et al., 1987; Sengupta et al., 1990; Waters, 1991; Dasgupta et al., 1995; Ouzegane and Boumaza, 1996; Ishii et al.,

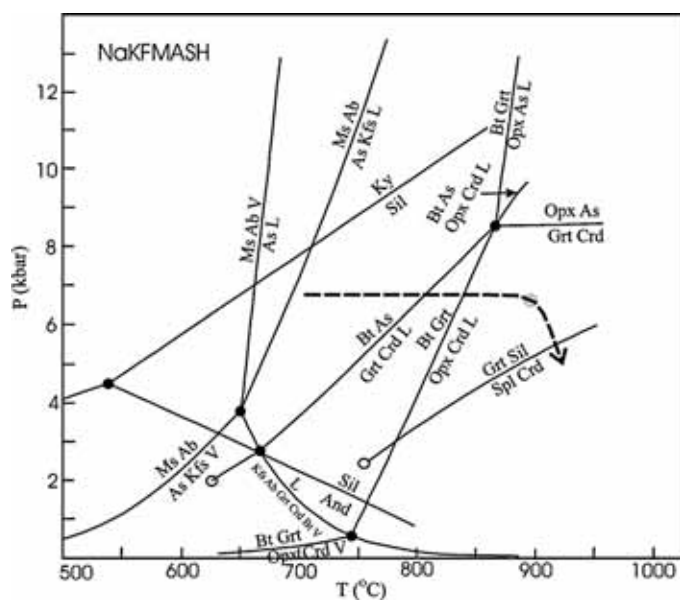


Fig. 7. Pressure–temperature diagram, showing possible P – T evolutionary path, of the studied pelitic granulite with reference to the simplified petrogenetic grid in the system NaKFMASH (after Spear et al., 1999). Small fill circle on the PT path indicates the peak PT condition.

2006; Santosh et al., 2006a,b; Shimizu et al., 2009). This assemblage is indicative of UHT metamorphism but may not be used as diagnostic for UHT as discussed extensively by several workers (Harley, 2008 and references therein). The principal reason lies in the dependence of the stability of spinel on Zn, Cr and Fe^{3+} . It is noted in this context that spinel in the studied granulites contains substantial amount of Zn. Stability of spinel-bearing assemblages will be enlarged at high fO_2 as argued by Hensen (1986). Zn has a similar role to Fe^{3+} and at temperatures $\leq 850^\circ C$, Zn is more influential than Fe^{3+} to stabilise spinel bearing assemblages (Sengupta et al., 1991; Dasgupta et al., 1995). A garnet–spinel–cordierite assemblage with K-feldspar, quartz and liquid is also stabilised at relatively low pressures and high temperatures in the system NKFMAH according to Spear et al. (1999). This simplified quantitative petrogenetic grid demonstrates that the development of retrograde spinel and cordierite (reactions (3)–(5)) is related to decompression subsequent to peak metamorphism (Fig. 7).

4. Zircon U–Pb Sensitive High Resolution Ion Microprobe (SHRIMP) study

For the first time, a systematic geochronological study is presented on the pelitic granulites and granites to ascertain the age of the granulite-grade part of the South Delhi Terrane as well as explain the dynamics of juxtaposition with the low-grade part of the South Delhi Terrane. Though some isotopic dates are available in the literature, they were obtained from samples collected without an adequate understanding of their position with respect to the dynamics of the area. The present geochronological study focuses on zircons separated from pelitic granulites and various granitoid rocks. The former were dated to elucidate the sedimentation–deformation–metamorphic history of the basin, while the granites (G1, G2 and G3) are correlated with particular geological events revealed through detailed structural mapping.

4.1. Analytical technique

Zircon grains were extracted from fresh rock samples following standard mineral separation techniques and then hand picked

and mounted in epoxy resin together with zircon standard BR266 (Stern, 2001), TEMORA-2 (Black et al., 2004) and CZ3 (Pidgeon et al., 1994). The grains were studied applying carbon coating under JEOL-6400 SEM fitted with a cathode-luminescence (CL) detector; imaging was conducted at a working distance of 39 mm and using an accelerating voltage of 15 keV and beam current of ~ 5 nA. Identification of grains was done by back-scatter electron imaging and energy dispersive spectrometry. CL imaging was done to reveal internal structure and growth patterns (Corfu et al., 2003). (The CL images are stored as Fig. 10 in the Journal web site). Subsequently, the carbon coating was removed and a thin layer of ultra-pure gold coating applied. SHRIMP analysis was done following method described by Claoué-Long (1994). Working conditions included a primary beam current of 2–3 nA, slightly elliptical spot size of ~ 25 – $30 \mu m$, sensitivity of >20 counts per ppm Pb and per nA primary beam current, and a mass resolution of >4500 . Measurements were conducted on Zr_2O^+ , $^{204}Pb^+$, background, $^{206}Pb^+$, $^{207}Pb^+$, $^{208}Pb^+$, $^{238}U^+$, $^{232}ThO^+$ and $^{238}UO_2^+$ in sets of six scans, with a total analysis time of about 15 min per sample spot. Analyses of unknown and BR266 standard zircon were interspersed at a ratio 3:1, allowing calibration of $^{238}U/^{206}Pb$ ratios and U content using an age of 559 Ma and U content of 909 ppm (Stern, 2001). TEMORA-2 and CZ3 were used as control standards and yielded $^{206}Pb/^{238}U$ ages within error of those reported for them (Pidgeon et al., 1994; Black et al., 2004).

Common Pb correction is based on measured non-radiogenic ^{204}Pb isotope, and a common Pb composition applied following the Pb-evolution model of Stacey and Kramers (1975). The samples were analysed during two sessions, sample TB-2 in session 1, and the remaining samples in session 2. Standard calibration errors are reported in Table 2, but were not included in single spot ages and pooled age calculations. Single spot ages are reported at 1σ confidence level, while pooled ages are reported at 95% confidence (Fig. 8).

4.2. Sample no. TB-1

The sample was collected from a microgranite pluton belonging to the G3 phase of Ambaji granites west of Ghoda (Fig. 2). The granite is medium grained and pink coloured, and is considered to be synkinematically emplaced during the F_3 folding event, thus it defines the last major magmatic event in the South Delhi Terrane. Zircon from the sample ranges in size from 50 to $300 \mu m$, and have aspect ratios between 1:1 and 4:1. CL imaging reveals variable CL-response, with some zircon showing internal zoning patterns, some not. The main population represents euhedral and low to medium-CL grains, while a few rounded or irregular well-zoned bright-CL zircons probably represent a xenocrystic component. Many data points recorded high counts on ^{204}Pb , interpreted to indicate high proportions of non-radiogenic Pb related to high U content and resulting radiogenic damage (Table 2). These analyses were aborted after the first scan and not further discussed here. One analysis on a large, bright-CL zircon resulted in an age of 3195 Ma, and this grain is interpreted as a Mesoarchaean xenocryst. The main population of analyses, conducted on euhedral dark or medium-CL grains defines a weighted mean $^{206}Pb/^{238}U$ age of 759 ± 6 Ma, interpreted to record the emplacement age of the microgranite (Fig. 8). A similar age has been obtained for hypersthene bearing granites (758 Ma, Roy et al., 2005) as well as the Erinpura granites (735 Ma, Crawford, 1975) and Malani granites (ca. 771 Ma, Gregory et al., 2009) from the Marwar Craton.

4.3. Sample nos. TB-2 and TB-3

These samples were collected from pelitic granulites close to Surpagla (Fig. 2). Many zircon grains contain pleochroic halos in

Table 2
Zircon U–Pb SHRIMP data for samples from the Baram–Kui–Surpaga–Kengora area, South Delhi Terrane.

Spot name	f ₂₀₆ (%)	U (ppm)	Th	Th/U ($\pm 1\sigma$ abs)	(²³⁸ U/ ²⁰⁶ Pb) _{total} ($\pm 1\sigma$ Ma)	(²⁰⁷ Pb/ ²⁰⁶ Pb) _{total}	(²³⁸ U/ ²⁰⁶ Pb) ₂₀₄	(²⁰⁷ Pb/ ²⁰⁶ Pb) ₂₀₄	²⁰⁶ Pb/ ²³⁸ U Age	²⁰⁷ Pb/ ²⁰⁶ Pb Age
Sample TB1-F3 microgranite (analyses conducted during a single session. 6 BR266 standard analyses yielded a 2 σ error of the mean of 0.94%)										
TB1-1-1	1.263	305	605	2.05	10.93837 \pm 0.11232	0.11232 \pm 0.00059	11.07829 \pm 0.11790	0.05041 \pm 0.00270	557 \pm 6	214 \pm 124
TB1-1-2	0.191	222	187	0.87	7.88942 \pm 0.08277	0.08277 \pm 0.00061	7.90449 \pm 0.08327	0.06447 \pm 0.00102	768 \pm 8	757 \pm 33
TB1-1-3	0.017	238	239	1.04	1.66254 \pm 0.01683	0.01683 \pm 0.00060	1.66283 \pm 0.01683	0.25155 \pm 0.00061	3035 \pm 25	3195 \pm 4
TB1-1-4.2	0.185	466	110	0.24	7.97363 \pm 0.07879	0.07879 \pm 0.00042	7.98841 \pm 0.07906	0.06347 \pm 0.00064	760 \pm 7	724 \pm 21
TB1-1-5	0.631	514	348	0.70	8.10129 \pm 0.07959	0.07959 \pm 0.00053	8.15275 \pm 0.08074	0.06165 \pm 0.00132	746 \pm 7	662 \pm 46
TB1-1-6	0.732	721	214	0.31	7.86049 \pm 0.07591	0.07591 \pm 0.00033	7.91845 \pm 0.07680	0.05931 \pm 0.00110	767 \pm 7	578 \pm 40
TB1-1-7	9.091	430	142	0.34	11.29425 \pm 0.11426	0.11426 \pm 0.00077	12.42374 \pm 0.15419	0.07057 \pm 0.01157	499 \pm 6	945 \pm 336
TB1-1-8	1.256	451	243	0.56	7.90639 \pm 0.07833	0.07833 \pm 0.00087	8.00693 \pm 0.08031	0.06212 \pm 0.00201	759 \pm 7	678 \pm 69
TB1-1-9	0.606	294	135	0.48	7.99528 \pm 0.08159	0.08159 \pm 0.00053	8.04404 \pm 0.08261	0.06085 \pm 0.00125	755 \pm 7	634 \pm 44
TB1-1-10	0.339	528	430	0.84	6.38840 \pm 0.06818	0.06818 \pm 0.00039	6.41012 \pm 0.06852	0.06860 \pm 0.00073	935 \pm 9	887 \pm 22
TB1-1-11	0.582	380	220	0.60	8.42004 \pm 0.34259	0.34259 \pm 0.00054	8.46933 \pm 0.34505	0.05956 \pm 0.00189	719 \pm 28	588 \pm 69
TB1-1-11.1	0.564	709	314	0.46	7.84167 \pm 0.19772	0.19772 \pm 0.00038	7.88615 \pm 0.19917	0.06293 \pm 0.00137	770 \pm 18	706 \pm 46
TB1-1-12	0.486	745	580	0.81	8.68903 \pm 0.21905	0.21905 \pm 0.00038	8.73150 \pm 0.22026	0.06142 \pm 0.00095	699 \pm 17	654 \pm 33
Sample TB2-pelitic granulites (analyses conducted during a single session. 18 BR266 standard analyses yielded a 2 σ error of the mean of 0.88%)										
TB1-2-1	0.135	410	74	0.19	4.66405 \pm 0.04565	0.08288 \pm 0.00036	4.67033 \pm 0.04574	0.08174 \pm 0.00048	1251 \pm 11	1239 \pm 12
TB1-2-2	0.216	876	456	0.54	4.55475 \pm 0.04412	0.09189 \pm 0.00026	4.56463 \pm 0.04426	0.09007 \pm 0.00050	1277 \pm 11	1427 \pm 11
TB1-2-3	0.127	612	446	0.75	3.64744 \pm 0.05706	0.09808 \pm 0.00033	3.65208 \pm 0.05714	0.09698 \pm 0.00042	1560 \pm 22	1567 \pm 8
TB1-2-4	0.080	824	546	0.68	3.58701 \pm 0.03787	0.09866 \pm 0.00057	3.58988 \pm 0.03791	0.09797 \pm 0.00059	1584 \pm 15	1586 \pm 11
TB1-2-5	0.127	1566	394	0.26	4.32576 \pm 0.04334	0.09239 \pm 0.00023	4.33128 \pm 0.04340	0.09131 \pm 0.00031	1339 \pm 12	1453 \pm 6
TB1-2-6	0.002	606	94	0.16	5.05609 \pm 0.07951	0.08261 \pm 0.00117	5.05620 \pm 0.07952	0.08259 \pm 0.00117	1163 \pm 17	1260 \pm 28
TB1-2-7	0.062	584	237	0.42	4.05740 \pm 0.04003	0.09441 \pm 0.00065	4.05992 \pm 0.04007	0.09388 \pm 0.00068	1419 \pm 13	1506 \pm 14
TB1-2-8	0.592	297	94	0.33	3.81051 \pm 0.03888	0.09673 \pm 0.00046	3.83320 \pm 0.03936	0.09163 \pm 0.00124	1494 \pm 14	1460 \pm 26
TB1-2-9	0.225	386	178	0.48	3.78398 \pm 0.09641	0.09807 \pm 0.00109	3.79252 \pm 0.09665	0.09614 \pm 0.00122	1509 \pm 34	1551 \pm 24
TB1-2-10	0.168	467	64	0.14	4.65258 \pm 0.11761	0.08214 \pm 0.00040	4.66043 \pm 0.11782	0.08071 \pm 0.00052	1253 \pm 29	1214 \pm 13
TB1-2-12	0.107	861	632	0.76	3.97526 \pm 0.10022	0.09675 \pm 0.00062	3.97953 \pm 0.10033	0.09583 \pm 0.00067	1445 \pm 33	1545 \pm 13
TB1-2-13	0.002	285	71	0.26	4.98810 \pm 0.12717	0.08320 \pm 0.00056	4.98821 \pm 0.12718	0.08318 \pm 0.00061	1178 \pm 27	1273 \pm 14
TB1-2-14	0.312	357	204	0.59	3.51034 \pm 0.08889	0.10242 \pm 0.00043	3.52132 \pm 0.08819	0.09973 \pm 0.00074	1611 \pm 36	1619 \pm 14
TB1-2-15	0.034	520	458	0.91	3.59098 \pm 0.09083	0.09855 \pm 0.00047	3.59220 \pm 0.09086	0.09825 \pm 0.00050	1583 \pm 36	1591 \pm 10
TB1-2-16	0.169	277	174	0.65	4.33217 \pm 0.11345	0.08630 \pm 0.00068	4.33949 \pm 0.11368	0.08486 \pm 0.00092	1337 \pm 32	1312 \pm 21
TB1-2-17	0.053	221	142	0.66	3.53879 \pm 0.09031	0.10016 \pm 0.00055	3.54065 \pm 0.09037	0.09970 \pm 0.00063	1604 \pm 36	1619 \pm 12
TB1-2-18	0.203	481	205	0.44	3.97308 \pm 0.10044	0.09647 \pm 0.00041	3.98114 \pm 0.10067	0.09474 \pm 0.00069	1445 \pm 33	1523 \pm 14
Sample TB3-Pelitic granulites										
TB1-3-3	-0.002	108985	16316	0.15	4.68130 \pm 0.11792	0.06620 \pm 0.00012	4.68120 \pm 0.11792	0.06622 \pm 0.00012	1248 \pm 29	813 \pm 4
TB1-3-4	-0.015	146691	62492	0.44	5.02793 \pm 0.12845	0.06442 \pm 0.00018	5.02718 \pm 0.12844	0.06455 \pm 0.00019	1170 \pm 27	760 \pm 6
TB1-3-5	-0.028	113698	18530	0.17	5.01088 \pm 0.12558	0.06519 \pm 0.00012	5.00949 \pm 0.12555	0.06543 \pm 0.00017	1173 \pm 27	788 \pm 5
TB1-3-6	-0.009	155863	25089	0.17	4.72987 \pm 0.11861	0.06626 \pm 0.00010	4.72944 \pm 0.11860	0.06634 \pm 0.00012	1236 \pm 28	817 \pm 4
Sample TB4-F2 granite (analyses conducted during a single session. 18 BR266 standard analyses yielded a 2 σ error of the mean of 0.88%)										
TB1-4-2	7.489	18	5	0.28	6.759089 \pm 0.20040	0.07898 \pm 0.00238	7.30627 \pm 0.22816	0.01291 \pm 0.01212	827 \pm 24	
TB1-4-3	11.460	13	3	0.25	6.693442 \pm 0.20836	0.09210 \pm 0.00300	7.55979 \pm 0.31662	0.00000 \pm 0.00000	801 \pm 32	
TB1-4-4	2.279	26	8	0.32	7.004342 \pm 0.19764	0.07372 \pm 0.00193	7.16772 \pm 0.21277	0.05454 \pm 0.00834	842 \pm 23	
TB1-4-5	0.695	93	63	0.70	2.166661 \pm 0.05602	0.16609 \pm 0.00088	2.18183 \pm 0.05648	0.15992 \pm 0.00163	2432 \pm 52	2455 \pm 17
TB1-4-6	2.349	39	12	0.32	6.86019 \pm 0.18776	0.07697 \pm 0.00221	7.02520 \pm 0.19711	0.05724 \pm 0.00615	858 \pm 23	
TB1-4-8	2.980	20	7	0.39	6.888795 \pm 0.20367	0.07455 \pm 0.00231	7.10036 \pm 0.23267	0.04930 \pm 0.01259	849 \pm 26	
TB1-4-10	1.138	58	30	0.54	7.012299 \pm 0.19903	0.07662 \pm 0.00128	7.09302 \pm 0.20601	0.06718 \pm 0.00540	850 \pm 23	
TB1-4-11	4.311	21	7	0.33	6.809512 \pm 0.19894	0.08106 \pm 0.00233	7.11629 \pm 0.23519	0.04432 \pm 0.01413	848 \pm 26	
Sample TB5-synsedimentary metarhyolites (analyses conducted during a single session. 18 BR266 standard analyses yielded a 2 σ error of the mean of 0.88%)										
TB2-5-1	0.022	432	337	0.81	6.03262 \pm 0.18861	0.07250 \pm 0.00042	6.03393 \pm 0.18866	0.07232 \pm 0.00045	989 \pm 29	995 \pm 13
TB2-5-2	0.060	482	379	0.81	6.10726 \pm 0.19087	0.07190 \pm 0.00041	6.11094 \pm 0.19100	0.07139 \pm 0.00051	977 \pm 28	969 \pm 14
TB2-5-3	-0.149	304	213	0.72	6.03022 \pm 0.18915	0.07134 \pm 0.00051	6.02128 \pm 0.18891	0.07258 \pm 0.00076	990 \pm 29	1002 \pm 21
TB2-5-4	0.164	365	275	0.78	6.07952 \pm 0.19039	0.07178 \pm 0.00047	6.08953 \pm 0.19071	0.07041 \pm 0.00057	980 \pm 28	940 \pm 17
TB2-5-5	0.209	1252	1300	1.07	6.06988 \pm 0.18925	0.07307 \pm 0.00036	6.08257 \pm 0.18966	0.07132 \pm 0.00052	981 \pm 28	967 \pm 15
TB2-5-6	0.498	501	376	0.77	6.34448 \pm 0.20564	0.07559 \pm 0.00042	6.37621 \pm 0.20675	0.07145 \pm 0.00100	939 \pm 28	970 \pm 28
TB2-5-7	0.439	608	476	0.81	6.21743 \pm 0.19457	0.07295 \pm 0.00075	6.24482 \pm 0.19547	0.06929 \pm 0.00103	958 \pm 28	907 \pm 31
TB2-5-8	0.505	348	256	0.76	6.33487 \pm 0.22652	0.07118 \pm 0.00078	6.36705 \pm 0.22778	0.06695 \pm 0.00130	940 \pm 31	836 \pm 40

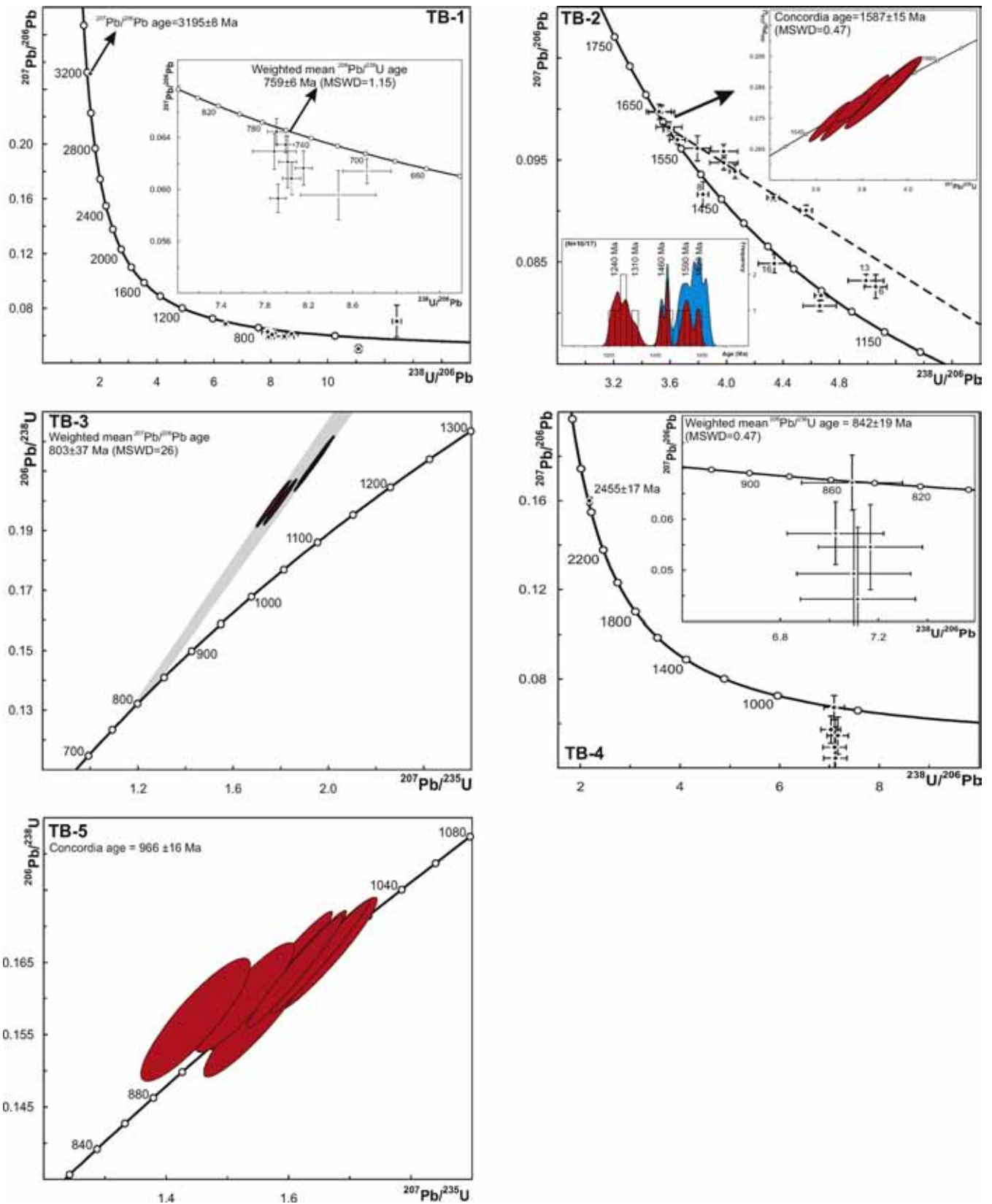


Fig. 8. Zircon U–Pb data for samples of the South Delhi Terrane from BSKK granulites. Error crosses are at 1σ confidence level. (For interpretation of the references to color in this figure legend, the reader is referred to the web version of the article.)

biotite, indicative of zircon inclusions with a high U content. Zircon from sample TB-2 range in size from 50 to 150 μm , and show rounded shapes indicative of a detrital origin. CL images show variable CL-response, with most zircon showing concentric zoning patterns indicating derivation from magmatic source rocks. Some zircons show narrow low-CL rim domains, possibly indicating zircon growth during a metamorphic event, but these were too small to allow analysis on SHRIMP. The zircon data in sample TB-2 show concordant crystallisation ages between 1591 and 1214 Ma (Table 2 and Fig. 8). An apparent coherent cluster of data appears to define a regression with an upper intercept at 1597 ± 23 Ma and lower intercept at 861 ± 83 Ma (MSWD=0.57), indicating a potentially homogeneous source rock of ca.1.6 Ga, and a Pb-loss event at ~ 860 Ma. The youngest detrital zircon grain in sample TB-2 recorded a concordant $^{207}\text{Pb}/^{206}\text{Pb}$ age of 1214 ± 25 Ma (2σ), which provides a maximum age of deposition for the metapelite protolith. Only four zircon crystals were analysed from sample TB-3, which turn out to have extremely high U contents of more than 100,000 ppm. These zircon crystals are extremely clear round crystals, interpreted to be of metamorphic origin. Because of their extremely high U content, the analyses plot inversely discordant, but define a narrow range of $^{207}\text{Pb}/^{206}\text{Pb}$ ratios corresponding to a weighted mean age of 803 ± 37 Ma. This age is within error of the lower intercept calculated from zircon analyses of sample TB-2, and supports a metamorphic event at ~ 800 Ma, inducing significant Pb-loss in detrital zircon in that sample. In summary, sedimentation in the South Delhi Terrane appears to be younger than 1214 ± 25 Ma and the sediments were metamorphosed to granulite facies probably at around 800 Ma. The analysed metapelite indicates sourcing from terranes with 1620, 1590, 1460, 1310 and 1240 Ma source rocks.

4.4. Sample no. TB- 4

The sample was collected from a coarse-grained granite (G2) that was emplaced synkinematically with F_2 folding, close to Surpagla (Fig. 2). The granite pluton occurs in the core of a large-scale F_2 fold. Zircon crystals from the sample range in size from 100 to 250 μm , and are generally elongate with aspect ratios greater than 2:1. The crystals are sub- to euhedral, and display well-developed zoning patterns typical for magmatic zircon. One rounded zircon analysis returned a Palaeoproterozoic $^{207}\text{Pb}/^{206}\text{Pb}$ age of 2455 ± 34 Ma and this grain is interpreted as a xenocryst. The main population of euhedral zircon records a weighted mean $^{206}\text{Pb}/^{238}\text{U}$ age of 842 ± 19 Ma interpreted to be the emplacement age of this S-type granitoid (Table 2, Fig. 8). Together with the evidence of metamorphism in samples TB-2 and TB-3, granulite facies metamorphism, granitisation of the sedimentary pile and synkinematic emplacement of the resulting S-type granitoids took place between 860 and 800 Ma. Previously determined ages for a granite gneiss of $836 + 7/-5$ Ma indicating peak metamorphism, and a monazite age of 826 ± 5 Ma suggesting cooling (Deb et al., 2001), match our results.

4.5. Sample no. TB-5

Sample TB-5 was collected from a metarhyolite, from the low-grade terrane, east of Surpagla (Fig. 2). The metarhyolite and pillowed-amphibolites form the alternate felsic and mafic lava flows in the basin, and have been deposited along with the sediments. Zircon crystals from the sample are euhedral and range in size from 100 to 200 μm , with length to width ratios between equant and 2:1. CL-imaging reveals broad zoning patterns consistent with magmatic growth. The zircon analyses define a concordia age of 966 ± 16 Ma taken as the extrusion age of the rhyolite and in-extenso, the deposition age of the succession at that level (Table 2,

Fig. 8). This depositional age is in agreement with the maximum age of deposition defined from the youngest concordant detrital grain in sample TB-2 (1214 ± 25 Ma). Given the deformation of the succession at 842 ± 19 Ma defined from the synkinematic G2 granite (Sample TB-4), an age bracket of 966–840 Ma can be suggested for the succession. This matches with the ages reported by Deb et al. (2001) for metarhyolites elsewhere in the region.

5. Discussion

5.1. Provenance, age of the deposition, deformation and metamorphism

The zircons in the pelitic granulites indicate granitic sources that show an age range between ca. 1620 and 1240 Ma. The areas directly adjoining the BSKS granulites are occupied by Erinpura granites and the Malani volcanic suite which have an age of ca. 750 Ma. The North Delhi Terrane further north comprises granites with Mesoproterozoic ages, which could have provided the source rocks for the detritus in BSKS protoliths (M-1, Table 1). However, recovery of 3195 Ma xenocrysts from sample TB-1 indicates that Mesoarchean basement rock might be hidden under alluvium and younger rocks of Marwar Craton.

Considering that the maximum age of deposition is ca. 1240 Ma and the age of the synsedimentary volcanism is 966 Ma, the onset of the sedimentation in the South Delhi Terrane could be constrained between 1240 and 966 Ma. The sedimentation would have continued until ca. 860 Ma, when deformation initiated with the closure of the basin through subduction followed by collision. The sediments were deformed and metamorphosed in granulite facies during the F_1 folding at 860 Ma. Hence, granulite metamorphism has occurred in a compressional setting. The granulites have been exhumed and juxtaposed against the low-grade rocks by thrusting before the F_3 folding event. The F_3 folding is well constrained by the emplacement of microgranite dykes at ca. 750 Ma. Hence formation and exhumation of the granulites occurs within an interval of 100 million years (860–750 Ma).

5.2. Comparison of the BSKS with others granulite terranes of the Indian Peninsula

The BSKS granulites are much younger than the granulites of the Sandmata Terrane (ca. 1.7 Ga, Dasgupta et al., 1997; Roy et al., 2005, see Fig. 9), the Saussar granulites of the Central India Mobile Belt (ca. 1.5 Ga, Sarkar et al., 1986, Acharyya and Roy, 2000; Bhowmik et al., 2005) and the Eastern Ghats Mobile Belt (ca. 1.6 and 1.0 Ga; cf. Dasgupta and Sengupta, 2003; Biswal et al., 2007). However, 795–740 Ma granulite facies metamorphism has been reported locally in the Chilka Lake area of the Eastern Ghats Mobile Belt (Krause et al., 2001; Dobmeier and Simmat, 2002). Major occurrences of granulites, close in age to the BSKS granulites, have been identified in the Southern Granulite terrane. The granulitic rocks in south India are divided into two blocks. The block north of the Salem–Attur–Palghat–Cauveri combined shear zone, called the Northern Granulite Terrane, is of Archaean age. There, magmatism has occurred at ca. 2530 Ma with subsequent high-grade metamorphism at ca. 2480 Ma (Peucat et al., 1993; Bhaskar Rao et al., 2003; Clark et al., 2009). The granulite terrane lying south of the above mentioned shear zone belongs to the Southern Granulite Terrane, and has been further divided into two blocks, namely the Madurai block and the Trivandrum block, separated by the Achankovil shear zone. The Madurai block is dominated by charnockites showing calc-alkaline affinity interpreted to reflect an arc setting (Santosh et al., 2009b). The charnockites and associated quartzites show HT

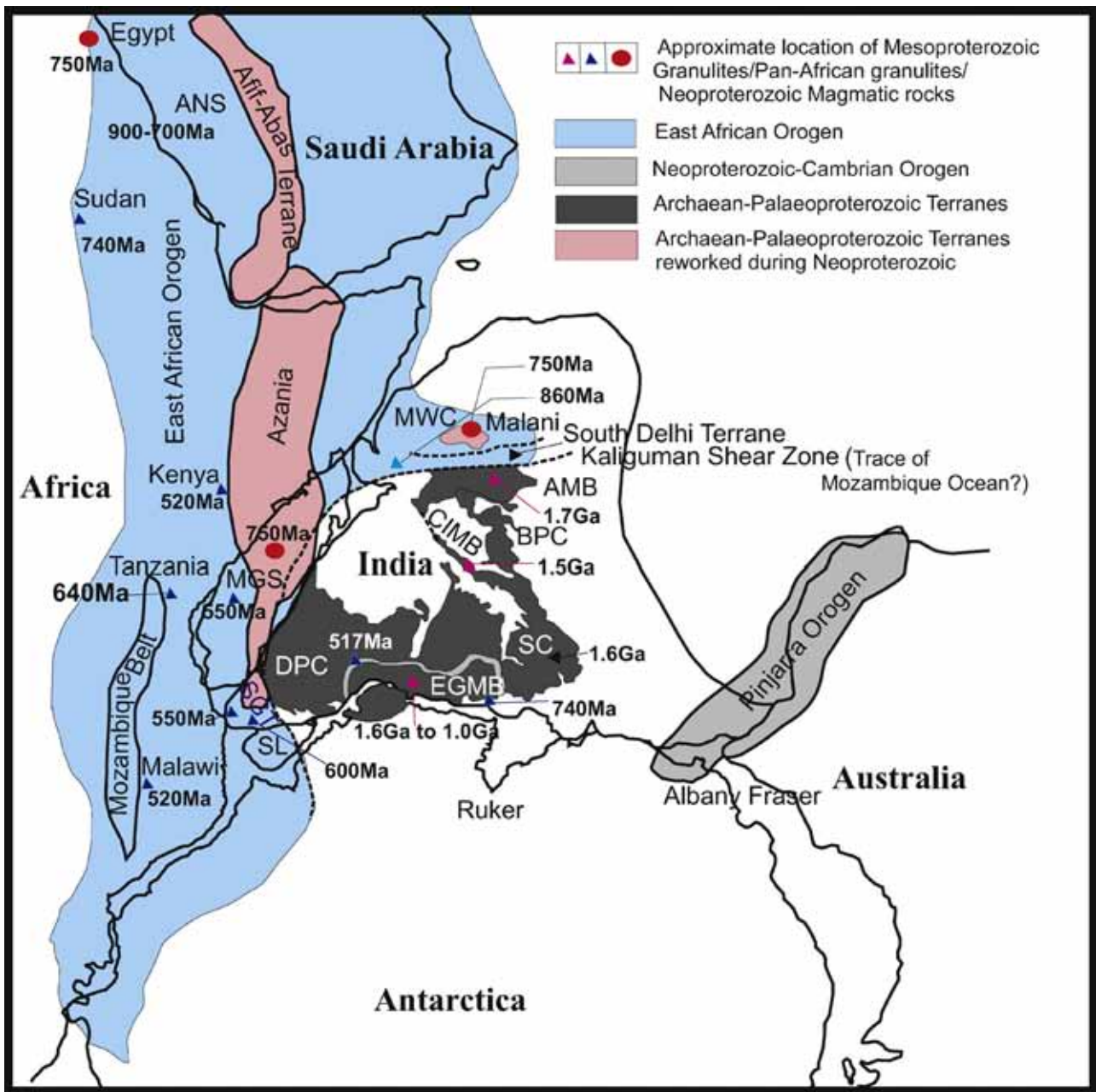


Fig. 9. Reconstruction of part of Gondwana showing various cratonic blocks after Fitzsimons (2003a,b), Johnson and Woldehaimanot (2003), Collins and Pisarevsky (2005) and Santosh et al. (2009a). ANS – Arabian-Nubian shield, AMB – Aravalli Mobile Belt, BPC – Bundelkhand Protocontinent, CIMB – Central India Mobile Belt, DPC – Dharwar Protocontinent, EGMB – Eastern Ghats Mobile Belt, MGS – Madagascar, MWC – Marwar Craton, SC – Singhbhum Craton, SGT – Southern Granulite Terrane, SL – Sri Lanka.

metamorphism (Sajeev et al., 2004) dated at 508 ± 9 Ma. Protolith ages are ca. 800–900 Ma. The charnockites are underlain by Palaeoproterozoic rocks (Collins et al., 2007b). The Trivandrum block is dominated by metasediments that show HT metamorphism at ca. 560–520 Ma (Santosh et al., 2006b). The Achankovil shear zone that separates the Madurai and Trivandrum block incorporates high-grade metamorphic rocks that record 8.5–9.0 kb and 940–1040 °C (Ishii et al., 2006). Metamorphic ages from the charnockites in the Achankovil shear zone range between 548 ± 2 and 526 ± 3 Ma (Ghosh et al., 2004). Because of the difference in age and metamorphic condition between the Northern Granulite and Southern Granulite terranes, the Salem–Attur–Palghat–Cauveri combined shear zone has been visualized as a Cambrian suture that resulted in the subduction of the northern block with closure of parts of the Mozambique ocean (Collins et al., 2007b; Santosh et al.,

2009b). Ophiolites and oceanic plagiogranites (Hussain et al., 1996; Santosh et al., 2009b), unusual Mg–Al rich mafic gneisses recording HP, 12 kb and UHT, 950 °C (Santosh et al., 2004; Santosh and Sajeev, 2006; Shimpo et al., 2006; Collins et al., 2007a; Tsunogae et al., 2008a,b) and garnet–omphacite–quartz bearing eclogite facies assemblages (Sajeev et al., 2009) have been reported from the shear zone. All these lines of evidences suggest a convergent tectonic regime where an ocean has been closed, and high-grade assemblages have been thrust up. Towards the north, the charnockites occur as thrust sheets emplaced over the Archaean basement, forming a fold- and thrust belt (Santosh et al., 2009b; Biswal et al., 2009). Available geochronological data, including U–Pb zircon and EPMA monazite ages, indicate that the rocks along the Palghat–Cauvery Shear Zone underwent an episode of high-grade metamorphism at ca. 530 Ma (Collins et al., 2007a; Santosh et al., 2006b). The

BKSK granulites show similarity with the Southern Granulites in that both owe their origin to compressional setting in a Precambrian subduction zone, exhumation through thrusting and a similar period of evolution.

The extension of the Salem–Attur–Palghat–Cauveri combined shear zone into Madagascar to the west and further west into the East African Orogen, and into Sri Lanka and Antarctica in the east has been proposed to suggest the presence of the Mozambique ocean, which closed due to collision between components of East and West Gondwana during the late-Neoproterozoic and early-Cambrian (Pan-African, Harris et al., 1994; Collins and Windley, 2002; Collins and Pisarevsky, 2005; Collins et al., 2007b; Santosh et al., 2009a; Naganjaneyulua and Santosh, 2010).

5.3. Comparison of the BKSK granulites with East African Orogen (EAO) granulites

The EAO occurs along the east coast of Africa and includes the Arabian-Nubian Shield (ANS), the Mozambique Belt and large parts of Madagascar (Fig. 9). The northern part of the EAO is occupied by the ANS exposed on either side of the Red Sea and covering Saudi Arabia, Egypt, Ethiopia and Sudan. The ANS in Saudi Arabia is comprised of juvenile crust formed by the consolidation of several arc/back-arc basin systems, involving abundant ophiolites, calc-alkaline arc volcanics and plutonic sequences (granite, granodiorite, tonalite and trondhjemite, dioritic rocks, alkali granite, aluminous granite, syenite and gabbro) and volcanogenic sediments. These rocks range in age between 825 and 565 Ma (Stoesser, 1986; Stern, 1994, 2002; Johnson and Woldehaimanot, 2003; Hargrove et al., 2006). The early Proterozoic-Archaean (2840 Ma) as well as Mesoproterozoic crust (1029 Ma) components have been reported from the ANS to be thermotectonically reworked (Be'eri-Shlevin et al., 2009). From the adjoining terranes of Egypt, Neoproterozoic to Cambrian volcanism has been reported, e.g. large-scale intrusion of ca. 750 Ma volcanic rocks (Ali et al., 2009) and 550–530 Ma post-orogenic granites from Ethiopia (Kröner et al., 2001). Greenschist to amphibolite facies metamorphism has been recorded in the rocks of the ANS that suggests that the northern part of the EAO represents the upper crustal section of the orogen. However, the EAO southward shows increase in the grade of metamorphism as in the Jebel Moya area of Sudan where charnockites and enderbites are reported. These are produced from granulite facies metamorphism of juvenile granitic protolith emplaced at ca. 742 Ma (Stern and Dawoud, 1991). The Mozambique Belt along the eastern margin of the Tanzania Craton is characterized by ca. 815 Ma granites, anorthosites and mafic rocks that have been metamorphosed to granulite facies at 640 Ma. Garnet–orthopyroxene–clinopyroxene–plagioclase–quartz in mafic granulites indicates peak metamorphic conditions of 9.5–11.0 kb and 800 °C and an anticlockwise PT path (Meert et al., 1995; Herms and Schenk, 1998; Maboko and Nakamura, 2002; Kröner et al., 2003). An anticlockwise PT path suggests magmatic underplating to be the cause of granulite facies metamorphism, arguing against the continental collision model suggested for other granulites of the EAO (Appel et al., 1998). A clockwise path is reported from the EAO exposed in Kenya (Bauernhofer et al., 2008 and references therein) as well as from Malawi (Kröner et al., 2001). At Taita Hills in Kenya, the rocks comprising migmatites, mafic granulites and marble show a two-stage granulite event. The peak metamorphism with PT at 10–12 kb, 760–840 °C has occurred at 644 Ma, and was followed by a second event at 550 Ma. The rocks have suffered thrust tectonics and have undergone multiple collisions during ~800 Ma and ~550 Ma. In Mozambique the eastern granulite belt has been thrust over western Mesoproterozoic terranes (the Nampula Belt, see Bingen et al., 2009)

as nappes. These granulitic nappes reflect arc-derived lithologies, with emplacement ages of 841–632 Ma. In Malawi a Pan-African period of intrusion of calc-alkaline granitoids around 710–555 Ma and a long-lasting thermal peak of Pan-African high-grade metamorphism around 571–549 Ma has been noted (Kröner et al., 2001). Madagascar consists of a collage of terranes showing a diverse tectonic history. Granulite facies metamorphism in the central part of the island occurred at between 550 and 530 Ma (e.g. Kröner et al., 2000). The northern part of Madagascar records sillimanite–garnet–biotite–orthoclase–cordierite granulites that record an isothermal decompression-type path, at pressures of 6.5–8.5 kb and temperatures between 800 and 900 °C. This metamorphism occurred at ca. 510–520 Ma (Buchwaldt et al., 2003; Jöns et al., 2006). In the south, sapphirine–kornferupine granulites show isothermal decompression at pressures of over 10 kb and temperatures between 700 and 800 °C, with exhumation recorded at 550 Ma (Razakamananal et al., 2001). From the above discussion it is apparent that the BKSK granulites are similar in age as well as structural style with the various granulite belts of the EAO. High-grade metamorphism in a compressional setting, exhumation through thrusting and Neoproterozoic magmatism are common to all these belts.

The geological make-up of Sri Lanka is still controversial. It comprises a 1.0 Ga terrane, the Wannu Complex, and a Palaeoproterozoic terrane, the Vijayan Complex with the central Highland Complex dated at ca. 2.0 Ga. These terranes were juxtaposed to the Southern Granulite Terrane of India at around 550 Ma (Kehelpannala, 2004). Spinel–sapphirine–cordierite granulites of the Highland Complex show conditions of ~9 kb at ~830 °C and isothermal decompression, with metamorphic ages of 610–550 Ma (Kriegsman and Schumacher, 1999). The variability of peak metamorphic ages throughout the orogen suggests that the EAO was formed through a succession of collisional and accretionary events in the Neoproterozoic.

6. Tectonic model

Our structural, metamorphic and geochronological studies indicate that the Delhi granulites are early to mid-Neoproterozoic in age (~900–700 Ma). Although a late-Neoproterozoic–early-Cambrian overprint is not very prominent, the brittle deformation and pseudotachylite formation in the granulites have been envisaged to be Neoproterozoic–Cambrian in age (Sarkar and Biswal, 2005). An isolated biotite age of 535 ± 15 Ma from the Ambaji granites also supports thermal reworking in the early-Cambrian (Crawford, 1975).

In the Gondwana reconstruction, NW India lies proximal to the EAO (Fig. 9). Magmatism at around 750 Ma is present in India (Malani Igneous suite), Madagascar and the Seychelles (Tucker et al., 2001; Ashwal et al., 2002; Kochhar, 2008; Thomas et al., 2009) and the ANS (Stern and Dawoud, 1991). Based on the similarity in geochemistry of the ~750 Ma granites, Kochhar (2008) proposed a Malani supercontinent consisting of India, ANS, Madagascar and China. Torsvik et al. (1999) indicated close similarity in palaeopole position between NW India and the Seychelles during that period. Archaean basement has been identified in the Affif-Abas terrane of the Arabian-Nubian shield (ANS), and central Madagascar, and these Archaean components could either be microcontinental blocks (e.g. Azania, after Collins and Pisarevsky, 2005) or be remnant of extensions to the Tanzania, Dharwar or the Marwar Cratons that formed part of the Malani supercontinent (Fig. 9). However, geochemistry and isotopic data for northern Madagascar and the Seychelles (Tucker et al., 1999; Thomas et al., 2009) clearly demonstrate these to represent juvenile (oceanic) arcs.

In view of the similarity between the South Delhi Terrane and the components of the EAO, it is proposed that the South Delhi Terrane marks a suture zone between western components including East Africa, Madagascar and the ANS, intervening oceanic arcs such as the Bemarivo Belt of northern Madagascar and the Seychelles, and eastern components including the Dharwar–Marwar Craton and the Aravalli Mobile belt–Bundelkhand Protocontinent. The South Delhi basin may be a remnant of the proto-Mozambique Ocean in NW India (Fig. 9). The basin closed through subduction, sediments were metamorphosed to granulite facies and the granulites were exhumed through thrusting during Neoproterozoic times.

The absence of 560–520 Ma metamorphism (or at least the localised and minor impact of such events), in the Seychelles and South Delhi Terrane, indicate that those terranes were distal to the collisional front of the EAO. This would be consistent with a model in which the Bemarivo Belt would have been attached to the Seychelles and South Delhi Terrane (and Dharwar–Marwar), and formed the frontal part of the collision, while inboard areas (Seychelles, South Delhi Terrane) only showed some far-field effects. The suture then records the soft collision of the Bemarivo and Seychelles oceanic arcs to India at around 750 Ma. This collage (from West to East, Bemarivo, Seychelles, South Delhi Terrane, Marwar Craton) then collided to Madagascar in the EAO at between 560 and 530 Ma (Buchwaldt et al., 2003; Jöns et al., 2006; ‘Malagasy orogeny’ Collins, 2006). Then, as Gondwana broke up, portions were left attached to Madagascar (the Bemarivo Belt), portions detached from everything and left in the developing Indian Ocean (the Seychelles) and one part, the South Delhi Terrane, was left attached to India.

The inset in Fig. 1a shows the Aravalli Mobile Belt to be curved eastward to join the Central India Mobile Belt (Naqvi and Rogers, 1987). This has been done on the assumption that the Aravalli Mobile belt represents a Mesoproterozoic terrane comparable with other mobile belts in India. However, our new data indicate that the South Delhi Terrane is Neoproterozoic in age. We therefore suggest that the Kaliguman shear zone (K, Fig. 1a, 1b, Fig. 9) that demarcates the boundary between South Delhi Terrane and the Aravalli–Bhilwara terrane (Fig. 1) marks a suture line along which the South Delhi basin closed through subduction (Sugden et al., 1990; Biswal et al., 1998a). Thus the Aravalli Mobile Belt could be divided by the Kaliguman Shear Zone into an easterly Mesoproterozoic and a westerly Neoproterozoic terrane. The Neoproterozoic terranes, namely the South Delhi Terrane and Sirohi Terrane, would extend southwestward and join with similar terranes of the EAO (Vijaya Rao et al., 2000). Work from the Eastern Ghats Mobile Belt, Southern Granulite Terrane and Aravalli Mobile Belt shows that the Indian Peninsula was not a coherent block until the Neoproterozoic but that various crustal blocks finally amalgamated during the late-Neoproterozoic–Cambrian “Pan-African” period (Mezger and Cosca, 1999; Biswal et al., 2007; Gregory et al., 2009). The suturing of the Africa–ANS with the Indian Peninsula along the South Delhi Terrane is therefore a significant event in the build up of Greater India during the Neoproterozoic period.

Acknowledgements

We sincerely thank the Department of Science and Technology, New Delhi and Indian Institute of Technology, Bombay for financial help. The EPMA analysis was done in Indian Institute of Technology, Roorkee and SHRIMP analyses conducted at the Perth Consortium facility at Curtin University of Technology (John de Laeter Centre for Excellence in Mass Spectrometry). CL imaging was conducted at the Centre for Microscopy and Microanalysis at the University of Western Australia. Discussions held with Profs. S. Dasgupta and

A.B. Roy during the preparation of this manuscript have greatly improved this work. Reviews by Profs. M. Santosh, Alan Collins and P. Cawood are heartily acknowledged.

Appendix A. Supplementary data

Supplementary data associated with this article can be found, in the online version, at doi:10.1016/j.precamres.2010.08.005.

References

- Acharyya, S.K., Roy, A., 2000. Tectonothermal history of the Central Indian Tectonic Zone and reactivation of Major Faults/Shear zones. *Journal of Geological Society of India* 55, 239–256.
- Ali, K.A., Stern, R.J., Manton, W.I., Kimura, J., Khamees, H.A., 2009. Geochemistry, Nd isotopes and U–Pb SHRIMP zircon dating of Neoproterozoic volcanic rocks from the Central Eastern Desert of Egypt: new insights into the 750 Ma crust-forming event. *Precambrian Research* 171, 1–22.
- Anbazhagan, S., Biswal, T.K., Roy, T., Kusuma, K.N., 2006. Remote sensing study of the granulite terrain in part of Gujarat and Rajasthan. *Journal of Indian Society of Remote Sensing* 34, 331–334.
- Appel, P., Moller, A., Schenk, V., 1998. High-pressure granulite facies metamorphism in the Pan-African belt of eastern Tanzania: *P–T–t* evidence against granulite formation by continent collision. *Journal of Metamorphic Geology* 16, 491–509.
- Ashwal, L.D., Demaiffe, D., Torsvik, T.H., 2002. Petrogenesis of Neoproterozoic granulites and related rocks from the Seychelles: the Case for an Andean-type Arc origin. *Journal of Petrology* 43, 45–83.
- Bauernhofer, A.H., Hauzenberger, C.A., Wallbrecher, E., Hoinkes, G., Muhongo, S., Mathu, E.M., 2008. Pan-African deformation in SE Kenya and NE Tanzania: geotectonic implications for the development of the North-Central Mozambique Belt. *African Journal of Science and Technology* 9, 50–71.
- Be’eri-Shlevin, Y., Katzir, Y., Whitehouse, M., 2009. Post-collisional tectonomagmatic evolution in the northern Arabian–Nubian Shield: time constraints from ion-probe U–Pb dating of zircon. *Journal of Geological Society of London* 166, 71–85.
- Bhaskar Rao, Y.J., Janardhan, A.S., Vijaya Kumar, T., Narayana, B.L., Dayal, A.M., Taylor, P.N., Chetty, T.R.K., 2003. Sm–Nd model ages and Rb–Sr isotopic systematics of charnockites and gneisses across Cauvery shear zone, Southern India: implication for the Archaean–Neoproterozoic Terrane Boundary in the Southern Granulite Terrane. *Memoir Geological Society of India* 50, 297–317.
- Bhattacharya, A., Mazumdar, A.C., Sen, S.K., 1988. Fe–Mg mixing in cordierite: constraints from natural data and implications for cordierite–garnet thermometry in granulites. *American Mineralogist* 73, 338–344.
- Bhattacharya, S., Sen, S.K., Acharyya, A., 1994. The structural setting of the Chilka Lake granulite–migmatite–anorthosite suite with emphasis on the time relation of charnockites. *Precambrian Research* 66, 393–409.
- Bhowmik, S.K., Basu Sarbadhikari, A., Spiering, B., Raith, M.M., 2005. Mesoproterozoic reworking of palaeoproterozoic ultrahigh temperature granulites in the central Indian tectonic zone and its implications. *Journal of Petrology* 46, 1085–1119.
- Bhushan, S.K., 2000. Malani rhyolites—a review. *Gondwana Research* 3, 65–77.
- Bingen, B., Jacobs, J., Viola, G., Henderson, I.H.C., Skår, Ø., Boyd, R., Thomas, R.J., Solli, A., Key, R.M., Daudi, E.X.F., 2009. Geochronology of the Precambrian crust in the Mozambique belt in NE Mozambique, and implications for Gondwana assembly. *Precambrian Research* 170, 231–255.
- Biswal, T.K., 1988. Polyphase deformation in Delhi rocks, south-east Amirgarh, Banaskantha district, Gujarat, in Precambrian of the Aravalli Mountain, Rajasthan, India. *Memoir Geological Society of India* 7, 267–277.
- Biswal, T.K., De Waele, B., Ahuja, H., 2007. Timing and dynamics of the juxtaposition of the Eastern Ghats Mobile Belt against the Bhandara Craton, India: a structural and zircon U–Pb SHRIMP study of the fold–thrust belt and associated nepheline syenite. *Tectonics* 26, TC4006, doi:10.1029/2006TC002005.
- Biswal, T.K., Gyani, K.C., Parthasarathy, R., Pant, D.R., 1998a. Tectonic implication of geochemistry of gabbro–norite–basic granulite suite in the Proterozoic Delhi Supergroup, Rajasthan, India. *Journal of Geological Society of India* 52, 721–732.
- Biswal, T.K., Gyani, K.C., Parthasarathy, R., Pant, D.R., 1998b. Implications of the geochemistry of the Pelitic Granulites of the Delhi Supergroup, Aravalli Mountain Belt, Northwestern India. *Precambrian Research* 87, 75–85.
- Biswal, T.K., Sarkar, S., Pal, A., Chakraborty, U., 2004. Pseudotachylites of the Kui–Chitraseni shear zones of the Precambrian Aravalli Mountain, Rajasthan. *Journal of Geological Society of India* 64, 325–335.
- Biswal, T.K., Sinha, S., 2003. Deformation history of the NW salient of the Eastern Ghats Mobile Belt, India. *Journal of Asian Earth Science* 22, 157–169.
- Biswal, T.K., Thirukumaran, V., Ratre Kamleshwar, Sundaralingam, K., 2009. Study of the Salem–Attur shear zone, east of Salem, Tamil Nadu: a new kinematic interpretation. *Current Science* 96, 1386–1389.
- Black, L.P., Kamoc, S.L., Allen, C.M., Davis, D.W., Aleinikoff, J.N., Valley, J.W., Mundil, R., Campbell, I.H., Korsch, R.J., Williams, I.S., Foudoulis, C., 2004. Improved ²⁰⁶Pb/²³⁸U microprobe geochronology by the monitoring of a trace-element-related matrix effect; SHRIMP, ID-TIMS, ELA-ICP-MS and oxygen isotope documentation for a series of zircon standards. *Chemical Geology* 205, 115–140.
- Bose, U., Sharma, A.K., 1992. The volcano sedimentary association of the Precambrian Hindoli Supracrustals in the Southeast Rajasthan. *Journal of Geological Society of India* 40, 359–369.

- Buchwaldt, R., Tucker, R.D., Dymek, R.F., 2003. Geothermobarometry and U–Pb Geochronology of metapelitic granulites and pelitic migmatites from the Lokoho region, Northern Madagascar. *American Mineralogist* 88, 1753–1768.
- Choudhary, A.K., Gopalan, K., Sastry, C.A., 1984. Present status of the geochronology of the Precambrian rocks of Rajasthan. *Tectonophysics* 105, 131–140.
- Claué-Long, J., 1994. SHRIMP zircon data, p. 33.
- Clark, C., Collins, A.S., Timms, N.E., Kinny, P.D., Chetty, T.R.K., Santosh, M., 2009. SHRIMP U–Pb age constraints on magmatism and high-grade metamorphism in the Salem Block, southern India. *Gondwana Research* 16, 27–36.
- Collins, A.S., 2006. Madagascar and the amalgamation of Central Gondwana. *Gondwana Research (GR Focus)* 9, 3–16.
- Collins, A.S., Windley, B.F., 2002. The tectonic evolution of central and northern Madagascar and its place in the final assembly of Gondwana. *Journal of Geology* 110, 325–340.
- Collins, A.S., Pisarevsky, S.A., 2005. Amalgamating Eastern Gondwana: the evolution of the Circum-Indian Orogens. *Earth Science Reviews* 7, 229–270.
- Collins, A.S., Clark, C., Sajeev, K., Santosh, M., Kelsey, D.E., Hand, M., 2007a. Passage through India: the Mozambique ocean suture, high pressure granulites and the Palghat–Cauvery shear system. *Terra Nova* 19, 141–147.
- Collins, A.S., Santosh, M., Braun, I., Clark, C., 2007b. Age and sedimentary provenance of the southern granulites, South India: U–Th–Pb SHRIMP secondary ion mass spectrometry. *Precambrian Research* 155, 125–138.
- Corfu, F., Hanchar, J.M., Hoskin, P.W.O., Kinny, P.D., 2003. Atlas of zircon textures. In: Hanchar, J.M., Hoskin, P.W.O. (Eds.), *Zircon. Mineralogy Society of America Mineral and Geochemistry Reviews*, Washington, DC, pp. 468–500.
- Crawford, A.R., 1970. The Precambrian geochronology of Rajasthan and Bundelkhand, Northern India. *Canadian Journal of Earth Science* 7, 91–110.
- Crawford, A.R., 1975. Rb–Sr age determination for the Mount Abu Granite and related rocks of Gujarat. *Journal of Geological Society of India* 16, 20–28.
- Das, K., Dasgupta, S., Miura, H., 2003. An experimentally constrained Petrogenetic grid in the silica-saturated portion of the system KFMASH at high temperatures and pressures. *Journal of Petrology* 44, 1055–1075.
- Dasgupta, S., Sengupta, P., 2003. Indo–Antarctic correlation: a perspective from the Eastern Ghats Granulite Belt, India. In: Yoshida, M., Windley, B.F., Dasgupta, S. (Eds.), *Proterozoic East Gondwana: Supercontinent Assembly and Breakup*, 206. *Journal Geological Society of London Special Publication*, pp. 131–143.
- Dasgupta, S., 1995. Pressure–temperature evolutionary history of the Eastern Ghats Granulite Province: recent advances and some thoughts. *Memoir Geological Society of India* 34, 101–110.
- Dasgupta, S., Guha, D., Sengupta, P., Miura, H., Ehl, J., 1997. Pressure–temperature–fluid evolutionary history of the polymetamorphic Sandmata granulite complex, Northwestern India. *Precambrian Research* 83, 267–290.
- Dasgupta, S., Sengupta, P., Ehl, J., Raith, M., Bardhan, S., 1995. Reaction textures in a suite of spinel granulites from the Eastern Ghats Belt, India: evidence for polymetamorphism, a partial petro-genetic grid in the system KFMASH and the roles of ZnO and Fe₂O₃. *Journal of Petrology* 36, 435–461.
- Deb, M., Thorpe, R.L., 2001. Geochronological constraints in the Precambrian Geology of Northwestern India and their Metallogenic Implication. In: Deb, M., Goodfellow, W.D. (Eds.), *Pre-Seminar volume on International Workshop on Sediment-hosted Lead-Zinc Sulfide Deposit in the Northwestern Indian Shield, Delhi-Udaipur, India*, Prepared at Dept of Geology, Delhi University, New Delhi, pp. 137–152.
- Deb, M., Thorpe, R.L., Cumming, G.L., Wagner, P.A., 1989. Age, source and stratigraphic implication of Pb isotope data for conformable, sediment-hosted, base metal deposits in the Proterozoic Aravalli–Delhi Orogenic Belt, Northwestern India. *Precambrian Research* 43, 1–22.
- Deb, M., Thorpe, R.L., Krstic, D., Corfu, F., Davis, D.W., 2001. Zircon U–Pb and galena Pb isotope evidence for an approximate 1.0 Ga terrane constituting the western margin of the Aravalli–Delhi orogenic belt, northwestern India. *Precambrian Research* 108, 195–213.
- Desai, S.J., Patel, M.P., Merh, S.S., 1978. Polymetamorphites of Balamar–Abu Road area, north Gujarat and southwestern Rajasthan. *Journal of Geological Society of India* 19, 383–394.
- Dobmeier, C., Simmat, R., 2002. Post-Grenvillian transpression in the Chilka Lake area, Eastern Ghats Belt—implications for the geological evolution of peninsular India. *Precambrian Research* 113, 243–268.
- Du Toit, A.L., 1937. *Our Wandering Continents*. Oliver and Boyd, Edinburgh and London, 366 pp.
- Fareeduddin, Kröner, A., 1998. Single zircon age constraints on the evolution of Rajasthan granulite. In: P.B.S. (Ed.), *The Indian Precambrian*. Scientific Publishers India, Jodhpur, pp. 547–556.
- Fitzsimons, I.C.W., 2003a. Does the late Neoproterozoic Darling Fault Zone of Western Australia extend all the way to the Transantarctic Mountains? SGTSG Field meeting. Abstracts–Geological Society of Australia 72, 130 (Kalbarri).
- Fitzsimons, I.C.W., 2003b. Proterozoic basement provinces of southern and southwestern Australia, and their correlation with Antarctica. In: Yoshida, M., Windley, B.F., Dasgupta, S. (Eds.), *Proterozoic East Gondwana: Supercontinent Assembly and Breakup*. Special Publication Geological Society of London, pp. 93–130.
- Franke, W., 1993. The Saxonian granulites: a metamorphic core complex? *Geologische Rundschau* 82, 505–515.
- Ghosh, J.G., De Wit, M.J., Zartman, R.E., 2004. Age and tectonic evolution of Neoproterozoic ductile shear zones in the Southern Granulite Terrain of India, with implications for Gondwana studies. *Tectonics* 23, TC3006, doi:10.1029/2002TC001444.
- Gopalan, K., Macdougall, J.D., Roy, A.B., Murali, A.V., 1990. Sm–Nd evidence for 3.3 Ga old rocks in Rajasthan, northwestern India. *Precambrian Research* 48, 287–297.
- Gopalan, K., Trivedi, J.R., Balsubramaniam, M.N., Ray, S.K., Sastry, C.A., 1979. Rb–Sr geochronology of the Khetri Copper, Rajasthan. *Journal of Geological Society of India* 20, 450–456.
- Grant, J.A., 1985a. Phase equilibria in low-pressure partial melting of pelitic rocks. *American Journal of Science* 285, 409–435.
- Grant, J.A., 1985b. Phase equilibria in partial melting of pelitic rocks. In: Ashworth, J.R. (Ed.), *Migmatites*. Blackie, Glasgow, pp. 86–144.
- Gregory, L.C., Meert, J.G., Bingen, B., Pandit, M.K., Torsvik, T.H., 2009. Paleomagnetism and geochronology of the Malani Igneous Suite, Northwest India: implications for the configuration of Rodinia and the assembly of Gondwana. *Precambrian Research* 170, 13–26.
- Guha, D.B., Bhattacharya, A.K., 1995. Metamorphic evolution and high-grade reworking of the Sandmata Complex granulites. In: Gupta, K.R., Sinha-Roy, S. (Eds.), *Continental Crust of Northwestern and Central India*, 31. *Memoir Geological Society of India*, pp. 163–198.
- Gupta, B.C., 1934. The geology of the central Mewar. *Memoir Geological Survey of India* 65, 107–169.
- Gupta, S.N., Arora, Y.K., Mathur, R.K., Iqballuddin, Prasad, B., Sahai, T.N., Sharma, S.B., 1980. Lithostratigraphic Map of the Aravalli Region. Geological Survey of India Publication, Hyderabad.
- Handy, M.R., Franz, L., Heller, B., Janott, B., Zurbirgen, R., 1999. Multistage accretion and exhumation of the continental crust (Ivrea crustal section, Italy and Switzerland). *Tectonics* 18, 1154–1177.
- Hansen, E.C., Newton, R.C., Janardhan, A.S., 1984. Pressures–temperatures and metamorphic fluids across unbroken amphibolite to granulite facies transition in southern Karnataka, India. In: Kröner, A., Goodwin, A.M., Hanson, G.N. (Eds.), *Archaean Geochemistry*. Springer, Berlin, pp. 161–181.
- Hargrove, U.S., Stern, R.J., Kimura, J.L., Manton, W.I., Johnson, P.R., 2006. Juvenile is the Arabian–Nubian Shield? Evidence from Nd isotopes and pre-Neoproterozoic inherited zircon in the Bi'r Umq suture zone, Saudi Arabia. *Earth and Planetary Science Letters* 252, 308–326.
- Harris, N.B.W., Santosh, M., Taylor, P.N., 1994. Crustal evolution in South India: constraints from Nd isotopes. *Journal of Geology* 102, 139–150.
- Harley, S.L., 1985. Garnet–orthopyroxene bearing granulites from Enderby Land, Antarctica: metamorphic pressure–temperature–time evolution of the Archaean Napier Complex. *Journal Petrology* 26, 819–856.
- Harley, S.L., 2008. Refining the P–T records of UHT crustal metamorphism. *Journal of Metamorphic Geology* 26, 125–154.
- Hensen, B.J., 1986. Theoretical phase relations involving cordierite and garnet revisited: the influence of oxygen fugacity on the stability of sapphirine and spinel in the system Mg–Fe–Al–Si–O. *Contribution to Mineralogy and Petrology* 92, 362–367.
- Herms, P., Schenk, V., 1998. Fluid inclusions in high-pressure granulites of the Pan-African belt in Tanzania (Uluguru Mts): a record of prograde to retrograde fluid evolution. *Contribution to Mineralogy and Petrology* 130, 199–212.
- Heron, A.M., 1953. The geology of central Rajputana. *Memoir Geological Survey of India* 79, 492 pp.
- Hussain, S.M., Narayana, B.L., Naqvi, S.M., 1996. Plagiogranite differentiates from ultramafic–mafic–felsic suite along Cauvery Suture at Manamedu in the granulite terrain of South India. In: *Proceedings of the 9th Convention of Indian Geological Congress*, pp. 155–160.
- Ishii, S., Tsunogae, T., Santosh, M., 2006. Ultrahigh-temperature metamorphism in the Achankovil Zone: implications for the correlation of crustal blocks in southern India. *Gondwana Research* 10, 99–114.
- Johnson, P.R., Woldehaimanot, B., 2003. Development of the Arabian–Nubian Shield: perspectives on accretion and deformation in the northern East African Orogen and the assembly of Gondwana. In: Yoshida, M., Windley, B.F., Dasgupta, S. (Eds.), *Proterozoic East Gondwana: Supercontinent Assembly and Breakup*, 206. *Geological Society of London Special Publication*, pp. 289–325.
- Jöns, N., Schenk, V., Appel, P., Razakamanana, T., 2006. Two-stage metamorphic evolution of the Bemarivo Belt of northern Madagascar: constraints from reaction textures and in situ monazite dating. *Journal of Metamorphic Geology* 2006 (24), 10.
- Kaur, P., Chaudhri, N., Raczek, I., Kroner, A., Hofmann, A.W., 2009. Record of 1.82 Ga Andean-type continental arc magmatism in NE Rajasthan, India: insights from zircon and Sm–Nd ages, combined with Nd–Sr isotope geochemistry. *Gondwana Research* 16, 56–71.
- Kehelpannala, K.V.W., 2004. Arc accretion around Sri Lanka during the assembly of Gondwana. *Gondwana Research* 7, 1323–1328.
- Kelsey, D.E., 2008. On ultrahigh-temperature crustal metamorphism. *Gondwana Research* 13, 1–29.
- Khan, M.S., Smith, T.E., Raza, M., Huang, J., 2005. Geology, geochemistry and tectonic significance of mafic–ultramafic rocks of mesoproterozoic phulad ophiolite suite of South Delhi Fold Belt, NW Indian Shield. *Gondwana Research* 8, 553–566.
- Kochhar, N., 2008. A-type Malani magmatism: Signatures of the Pan-African Event in the NW Indian Shield and Assembly of the Late Proterozoic Malani Supercontinent, vol. 91. Geological Survey of India Special Publication, pp. 112–128.
- Krause, O., Dobmeier, C., Raith, M.M., Mezger, K., 2001. Age of emplacement of mafic-type anorthosites in the Eastern Ghats Belt, India: constraints from U–Pb zircon dating and structural studies. *Precambrian Research* 109, 25–38.
- Kriegsman, L.M., Schumacher, J.C., 1999. Petrology of Sapphirine-bearing and associated granulites from Central Sri Lanka. *Journal of Petrology* 40, 1211–1239.

- Kröner, A., Hegner, E., Collins, A.S., Windley, B.F., Brewer, T.S., Razakamanana, T., Pidgeon, R.T., 2000. Age and magmatic history of the Antananarivo Block, Central Madagascar, as derived from zircon geochronology and Nd isotopic systematic. *American Journal of Science* 300, 251–288.
- Kröner, A., Collins, A.S., Hegner, E., Willner, A.P., Muhongo, S., Kehelpannala, K.V.W., 2001. The East African Orogen: new zircon and Nd ages and implications for Rodinia and Gondwana supercontinent formation and dispersal. *Gondwana Research* 4, 179–181.
- Kröner, A., Muhongo, S., Hegner, E., Wingate, M.T.D., 2003. Single zircon geochronology and Nd isotopic systematics of Proterozoic high-grade rocks from the Mozambique belt of southern Tanzania (Masasi area): implications for Gondwana assembly. *Journal of Geological Society of London* 160, 745–757.
- Lal, R.K., Ackermann, D., Upadhyay, H., 1987. *P–T–X* relationships deduced from corona textures in sapphirine–spinel–quartz assemblages from Paderu, southern India. *Journal of Petrology* 28, 1139–1168.
- Le Breton, N., Thompson, A.B., 1988. Fluid-absent (dehydration) melting of biotite in metapelites in the early stages of crustal anatexis. *Contribution to Mineralogy and Petrology* 99, 226–237.
- Maboko, M.A.H., Nakamura, E., 2002. Isotopic dating of Neoproterozoic crustal growth in the Usambara Mountains of Northeastern Tanzania: evidence for coeval crust formation in the Mozambique belt and the Arabian-Nubian Shield. *Precambrian Research* 113, 227–242.
- Macdougall, J.D., Gopalan, K., Lugmair, G.W., Roy, A.B., 1983. The Banded Gneissic Complex of Rajasthan, India: Early Crust from Depleted Mantle at ~3.5 Ga? *Eos, Transactions. American Geophysical Union*, 64, 351 pp.
- McDade, P., Harley, S.L., 2001. A petrogenetic grid for aluminous granulite facies metapelites in the KFMASH system. *Journal of Metamorphic Geology* 19, 45–59.
- Meert, J.G., Van der Voo, R., Ayub, S., 1995. Paleomagnetic investigation of the Neoproterozoic Gagwe lavas and Mbozi complex, Tanzania and the assembly of Gondwana. *Precambrian Research* 74, 225–244.
- Meert, J., Lieberman, B.S., 2008. The Neoproterozoic assembly of Gondwana and its relationship to the Ediacaran–Cambrian radiation. *Gondwana Research* 14, 5–21.
- Mezger, K., Cosca, M., 1999. The thermal history of the Eastern Ghats Belt (India), as revealed by U–Pb and ⁴⁰Ar/³⁹Ar dating of metamorphic and magmatic minerals: implications for the SWEAT hypothesis. *Precambrian Research* 94, 251–271.
- Mukherjee, A., 1998. The Eastern Ghats type metamorphism. *Geological Survey of India Records* 44, 137–144.
- Mukhopadhyay, D., Bhattacharya, T., Chattopadhyay, N., Lopez, R., Tobisch, T.O., 2000. Anasagar gneiss: a folded granulite pluton in the Proterozoic South Delhi Folded Belt, Central Rajasthan. *Proceedings of the Indian National Science Academy* 109, 21–37.
- Mukhopadhyay, D., Chattopadhyay, N., Bhattacharya, T., 2010. Structural Evolution of a Gneiss Dome in the Axial Zone of the Proterozoic South Delhi Fold Belt in Central Rajasthan. *Journal of Geological Society of India* 75, 18–31.
- Murao, S., Deb, M., Takagi, T., Seki, Y., Pringle, M., Naito, K., 2000. Geochemical and geochronological constraints for tin polymetallic mineralization in Tosham area, Haryana, India. In: Deb, M. (Ed.), *Crustal evolution and metallogeny in northwestern Indian shield*. Narosa publishing house, New Delhi, pp. 43–442.
- Naganjaneyulua, K., Santosh, M., 2010. The Cambrian collisional suture of Gondwana in southern India: a geophysical Appraisal. *Journal of Geodynamics* 50, 256–267.
- Naha, K., Halyburton, R.V., 1974a. Early Precambrian stratigraphy of central and southern Rajasthan, India. *Precambrian Research* 1, 55–73.
- Naha, K., Halyburton, R.V., 1974b. Late stress systems deduced from conjugate folds and kink bands in the “Main Raialo Syncline” Udaipur district, Rajasthan India. *Bulletin Geological Society of America*, 85, 251–256.
- Naha, K., Majumdar, A., 1971a. Re-interpretation of the Aravalli basal conglomerate at Morrachana, Udaipur district Rajasthan, Western India. *Geological Magazine* 108, 111–114.
- Naha, K., Majumdar, A., 1971b. Structure of the Rajnagar marble band and its bearing on the Precambrian stratigraphy of central Rajasthan, Western India. *Geologische Rundschau* 60, 1550–1571.
- Naha, K., Mohanty, S., 1988. Response of basement and cover rocks to multiple deformations a study from the Precambrian of central Rajasthan, western India. *Precambrian Research* 42, 77–96.
- Naha, K., Roy, A.B., 1983. The problem of the Precambrian basement in Rajasthan, Western India. *Precambrian Research* 19, 217–223.
- Naha, K., Mukhopadhyaya, D.K., Mohanty, R., Mitra, S.K., Biswal, T.K., 1984. Significance of contrast in the early stages of the structural history of the Delhi and the pre-Delhi rock groups in the Proterozoic of Rajasthan, western India. *Tectonophysics* 105, 193–206.
- Naha, K., Mitra, S.K., Biswal, T.K., 1987. Structural history of the rocks of the Delhi Group around Todgarh, Central Rajasthan. *Indian Journal of Geology* 59, 126–156.
- Naqvi, S.M., Rogers, J.J.W., 1987. *Precambrian Geology of India*. Oxford University Press, New York, 223 pp.
- Nichols, G.T., Berry, R.F., Green, D.H., 1992. Internally consistent garnitic spinel–cordierite–garnet equilibria in the FMASHZn system: geothermobarometry and applications. *Contribution to Mineralogy and Petrology* 111, 362–377.
- Ouzegane, K., Boumaza, S., 1996. An example of ultrahigh-temperature metamorphism: orthopyroxene–sillimanite–garnet, sapphirine–quartz and spinel–quartz parageneses in Al–Mg granulites from In Hihau, In Ouzal, Hoggar. *Journal of Metamorphic Geology* 14, 693–708.
- Pandit, M.K., Carter, L.M., Ashwal, L.D., Tucker, R.D., Torsvik, T.H., Jamtveit, B., Bhushan, S.K., 2003. Age, petrogenesis and significance of 1 Ga granitoids and related rocks from the Sendra area, Aravalli Craton, NW India. *Journal of Asian Earth Science* 22, 363–381.
- Peucat, J.J., Mahabaleshwar, B., Jayananda, M., 1993. Age of younger tonalitic magmatism and granulitic metamorphism in the South India transition zone (Krishnagiri area): comparison with older Peninsular gneisses from the Gorur–Hassan area. *Journal of Metamorphic Geology* 11, 879–888.
- Pidgeon, R.T., Furfuro, D., Kennedy, A.K., Nemchin, A.A., Van Bronswijk, W., 1994. Calibration of zircon standards for the Curtin SHRIMP II. *US. Geological Survey Circular* 1107, 251.
- Porwal, A., Carranza, E.J.M., Hale, M., 2006. Tectonostratigraphy and base-metal mineralization controls, Aravalli province (western India): new interpretations from geophysical data analysis. *Reviews in Ore Geology* 29, 287–306.
- Pradhan, V.R., Meert, J.G., Pandit, M.K., Kamenova, G., Gregory, L.C., Malone, S.J., 2010. India's changing place in global Proterozoic reconstructions: a review of geochronological constraints and paleomagnetic poles from the Dharwar, Bundelkhand and Marwar cratons. *Journal of Geodynamics* 50, 224–242.
- Raja Rao, C.S., Poddar, B.C., Basu, K.K., Dutta, A.K., 1971. Precambrian stratigraphy of Rajasthan—a review. *Geological Survey of India Memoir* 101, 60–79.
- Razakamanana, T., Windley, B.F., Ackermann, D., 2001. Sapphirine–kornepine granulites from the Precambrian of Southern Madagascar: implications for the evolution of the deep crust in East Gondwana. *Gondwana Research* 4, 252–253.
- Roy, A.B., 1988. Stratigraphic and tectonic framework of the Aravalli Mountain Range. In: Roy, A.B. (Ed.), *Memoir Geological Society India. Precambrian of the Aravalli Mountain, Rajasthan, India*, pp. 33–75.
- Roy, A.B., Jakhur, S.R., 2002. *Geology of Rajasthan (Northwest India) Precambrian to recent*. Scientific Publishers, Jodhpur, India, 205 pp.
- Roy, A.B., Kröner, A., 1996. Single zircon evaporation ages constraining the growth of the Archaean Aravalli craton, northwestern India shield. *Geological Magazine* 133, 333–342.
- Roy, A.B., Kröner, A., Laul, V., Purohit, R., 2005. Single zircon dating of hypersthene bearing granulite from Balam–Abu Road area, southern part of the Aravalli Mountains. In: Thomas, H. (Ed.), *NW India—Implication for Malani Magmatism related thermal event, in Metamorphism and Crustal Evolution*. Atlantic Publishers and Distributors, New Delhi, pp. 339–346.
- Roy, A.B., Sharma, K.K., 1999. Geology of the region around Sirohi Town, western Rajasthan—a story of Neoproterozoic evolution of the Aravalli crust. In: Paliwal, B.S. (Ed.), *Geological Evolution of the Northwestern India*. Scientific Publishers, Jodhpur, India, pp. 19–33.
- Sajeev, K., Osanai, Y., Santosh, M., 2004. Ultrahigh-temperature metamorphism followed by two-stage decompression of garnet–orthopyroxene–sillimanite granulites from Ganguvarpatti, Madurai block, southern India. *Contribution to Mineralogy and Petrology* 148, 29–46.
- Sajeev, K., Windley, B.F., Connolly, J.A.D., Kon, Y., 2009. Retrogressed eclogite (20 kb, 1020 °C) from the Neoproterozoic Palghat–Cauvery suture zone, Southern India. *Precambrian Research* 171, 23–36.
- Sandiford, M., Powell, R., 1986. Deep crustal metamorphism during continental extension: modern and ancient examples. *Earth and Planetary Science Letters* 79, 151–158.
- Sandiford, M., Neall, F.B., Powell, R., 1987. Metamorphic evolution of aluminous granulites from Labwor Hills, Uganda. *Contribution to Mineralogy and Petrology* 95, 217–225.
- Santosh, M., Tsunogae, T., Koshimoto, S., 2004. First report of sapphirine-bearing rocks from the Palghat–Cauvery Shear Zone system, southern India. *Gondwana Research* 7, 620–626.
- Santosh, M., Sajeev, K., 2006. Anticlockwise evolution of ultrahigh-temperature granulites within continental collision zone in southern India. *Lithos* 92, 447–464.
- Santosh, M., Sajeev, K., Li, J.H., 2006a. Extreme crustal metamorphism during Columbia supercontinent assembly: evidence from North China Craton. *Gondwana Research* 10, 256–266.
- Santosh, M., Collins, A.S., Tamashiro, I., Koshimoto, S., Tsutsumi, Y., Yokoyama, K., 2006b. The timing of ultrahigh-temperature metamorphism in Southern India: U–Th–Pb electron microprobe ages from zircon and monazite in sapphirine-bearing granulites. *Gondwana Research* 10, 128–155.
- Santosh, M., Maruyama, S., Yamamoto, S., 2009a. The making and breaking of supercontinents: some speculations based on superplumes, super downwelling and the role of tectosphere. *Gondwana Research* 15, 324–341.
- Santosh, M., Maruyama, S., Sato, K., 2009b. Anatomy of a Cambrian suture in Gondwana: Pacific-type orogeny in southern India? *Gondwana Research* 16, 321–341.
- Sarkar, G., Burman, T.R., Corfu, F., 1989. Timing of continental arc-type magmatism in northwest India: evidence from U–Pb zircon geochronology. *Journal of Geology* 97, 607–612.
- Sarkar, S., Biswal, T.K., 2005. Tectonic Significances of fissure veins associated with pseudotachylites of the Kui–Chitraseni Shear Zone, Aravalli Mountain, NW India. *Gondwana Research* 8, 277–282.
- Sarkar, S.N., Trivedi, J.R., Gopalan, K., 1986. Rb–Sr whole rock and mineral isochron age of Tirodi Gneiss, Sauser Group, Bhandara District, Maharashtra. *Journal of Geological Society of India* 27, 30–37.
- Sen, S., 1981. Proterozoic paleotectonics in the evolution of crust and location of metalliferous deposits. *Quarterly Journal of Geological Mineralogical Metallurgical Society of India* 53, 162–185.
- Sengupta, P., Dasgupta, S., Bhattacharya, P.K., Fukuoka, M., Chakraborti, S., Bhowmick, S., 1990. Proliferation of imprints in the sapphirine granulites from Anantagiri, Eastern Ghats Mobile Belt, India. *Journal of Petrology* 31, 971–996.
- Sengupta, P., Karmakar, S., Dasgupta, S., Fukuoka, M., 1991. Petrology of spinel granulites from Araku, eastern Ghats, India, and a petrogenetic grid for

- sapphirine-free rocks in the system FMAS. *Journal of Metamorphic Geology* 9, 451–459.
- Sharma, R.S., 1988. Pattern of metamorphism in the Precambrian Rocks of the Aravalli Mountain Belt. *Memoir Geological Society of India (Precambrian of the Aravalli Mountain, Rajasthan, India)* 7, 33–75.
- Shimizu, H., Tsunogae, T., Santosh, M., 2009. Spinel + quartz assemblage in granulites from the Achankovil Shear Zone, southern India: implication for ultrahigh-temperature metamorphism. *Journal of Asian Earth Science* 36, 209–222.
- Shimpo, M., Tsunogae, T., Santosh, M., 2006. First report of garnet–corundum rocks from Southern India: implications for prograde high-pressure (eclogite–facies?) metamorphism. *Earth and Planetary Science Letters* 242, 111–129.
- Sinha-Roy, S., Malhotra, G., Mohanty, M., 1998. *Geology of Rajasthan*. *Journal of Geological Society of India*, 278 pp.
- Sivaraman, T.V., Odom, A.L., 1982. Zircon chronology of the Berach granite of Chitorgarh, Rajasthan. *Journal of Geological Society of India* 23, 575–577.
- Spear, F.S., Kohn, M.J., Cheney, J.T., 1999. *P–T* paths from anatectic pelites. *Contribution to Mineralogy and Petrology* 134, 17–32.
- Srikarni, C., Limaye, M.A., Janardhan, A.S., 2004. Sapphirine bearing granulites from Abu-Balaram area, Gujarat State: implications for India–Madagascar Connection. *Gondwana Research* 7, 1214–1218.
- Stacey, J.S., Kramers, J.D., 1975. Approximation of terrestrial lead isotopic evolution by a two-stage model. *Earth and Planetary Science Letters* 26, 207–221.
- Stern, R.A., 2001. A New Isotopic and Trace-element Standard for the Ion Microprobe: Preliminary Thermal Ionization Mass Spectrometry (TIMS) U–Pb and Electron-Microprobe Data. 2001-F1. Geological Survey of Canada, Ottawa, Ontario, Canada.
- Stern, R.J., 1994. Arc assembly and continental collision in the Neoproterozoic East African Orogen: implications for the consolidation of Gondwana. *Earth and Planetary Science Reviews* 22, 319–351.
- Stern, R.J., 2002. Crustal evolution in the East African Orogen: a neodymium isotopic perspective. *Journal of African Earth Science* 34, 109–117.
- Stern, R.J., Dawoud, A.S., 1991. Late Precambrian (740 Ma) Charnockites, enderbites and granites from Jebel Moya, Sudan: a link between the Mozambique belt and the Arabian–Nubian shield? *Journal of Geology* 99, 648–659.
- Stoeser, D.B., 1986. Distribution and tectonic setting of plutonic rocks of the Arabian Shield. *Journal of African Earth Science* 4, 21–46.
- Sugden, T.J., Deb, M., Windley, B.F., 1990. The tectonic setting of mineralisation in the Proterozoic Aravalli–Delhi orogenic belt, NW India. In: N.S.M. (Ed.), *Precambrian Continental Crust and Its Economic Resources*. Elsevier, New York, pp. 367–390.
- Thomas, R.J., De Waele, B., Schofield, D.I., Goodenough, K.M., Horstwood, M.S.A., Tucker, R., Bauer, W., Annels, A.E., Howard, K., Walsh, G., Rabarimana, M., Rafahatelo, J.M., Ralison, A.V., Randriamananjara, T., 2009. Geological evolution of the Neoproterozoic Bemarivo Belt, northern Madagascar. *Precambrian Research* 172, 279–300.
- Tobisch, O.T., Collerson, K.D., Bhattacharya, T., Mukhopadhyay, D., 1994. Structural relationship and Sm–Nd isotope systematics of polymetamorphic granitic gneisses and granitic rocks from central Rajasthan, India—implications for the evolution of the Aravalli craton. *Precambrian Research* 65, 319–339.
- Torsvik, T.H., Ashwal, L.D., Tucker, B.D., De Wit, M.J., Eide, E.A., 1999. Geochronology and paleomagnetism of Seychelles dykes; implications for Rodinia supercontinent paleogeography. In: Anonymous (Ed.), *European Union of Geosciences conference abstracts; EUG 10*. *Journal of Conference Abstracts*. Cambridge Publications, Cambridge, United Kingdom, 116 pp.
- Tsunogae, T., Santosh, M., Ohyama, H., Sato, K., 2008a. High-pressure and ultra high temperature metamorphism at Komateri, northern Madurai Block, southern India. *Journal of Asian Earth Science* 33, 395–413.
- Tsunogae, T., Santosh, M., Dubessy, J., 2008b. Fluid characteristics of high- to ultrahigh temperature metamorphism in southern India: a quantitative Raman spectroscopic study. *Precambrian Research* 162, 198–211.
- Tucker, R.D., Ashwal, L.D., Hamilton, M.A., Torsvik, T.H., Carter, L.M., 1999. Neoproterozoic silicic magmatism of northern Madagascar, Seychelles, and NW India: clues to Rodinia's assembly and dispersal. *Geological Society of American Abstract Programme* 31, 317.
- Tucker, R.D., Ashwal, L.D., Torsvik, T.H., 2001. U–Pb geochronology of Seychelles granulites: a Neoproterozoic continental arc fragment. *Earth and Planetary Science Letters* 187, 27–38.
- Van Lente, B., Ashwal, L.D., Pandit, M.K., Bowring, S.A., Torsvik, T.H., 2009. Neoproterozoic hydrothermally altered basaltic rocks from Rajasthan, northwest India: implications for late Precambrian tectonic evolution of the Aravalli Craton. *Precambrian Research* 170, 202–222.
- Verma, P.K., Greiling, R.O., 1995. Tectonic evolution of the Aravalli orogen (NW India): an inverted proterozoic rift basin? *Geologische Rundschau* 84, 683–686.
- Vielzeuf, D., Holloway, J.R., 1988. Experimental determination of the fluid-absent melting relations in the pelitic system. *Consequences for crustal differentiation*. *Contribution to Mineralogy and Petrology* 98, 257–276.
- Vielzeuf, D., 1983. The spinel and quartz associations in high grade xenoliths from Tallante (S.E. Spain) and their potential use in geothermometry and barometry. *Contribution to Mineralogy and Petrology* 82, 301–311.
- Vijaya Rao, V., Rajendra Prasad, B., Reddy, P.R., Tewari, H.C., 2000. Evolution of Proterozoic Aravalli Delhi Fold Belt in the northwestern Indian Shield from seismic studies. *Tectonophysics* 327, 109–130.
- Volpe, A.M., Macdougall, J.D., 1990. Geochemistry and isotopic characteristics of mafic (Phulad ophiolite) and related rocks in the Delhi Supergroup, Rajasthan, India: implications for rifting in the Proterozoic. *Precambrian Research* 48, 167–191.
- Waters, D.J., 1988. Partial melting and the formation of granulite facies assemblages in Namaqualand, South Africa. *Journal of Metamorphic Geology* 6, 387–404.
- Waters, D.J., 1991. Hercynite–quartz granulites: phase, and implications for crustal processes. *European Journal of Mineralogy* 3, 367–386.
- Weber, K., 1984. Variscan events: early Palaeozoic continental rift metamorphism and late Palaeozoic crustal shortening. In: Hutton, D.H.W., Sanderson, D.J. (Eds.), *Variscan Tectonics of the North Atlantic Region*. Blackwell, Oxford, pp. 3–22.
- Wiedenbeck, M., Goswami, J.N., 1994. High precision $^{207}\text{Pb}/^{206}\text{Pb}$ zircon geochronology using a small ion microprobe. *Geochimica Cosmochimica Acta* 58, 2135–2141.
- Wiedenbeck, M., Goswami, J.N., Roy, A.B., 1996a. An ion microprobe study of the single zircons from the Amet granite, Rajasthan. *Journal of Geological Society of India* 48, 127–137.
- Wiedenbeck, M., Goswami, J.N., Roy, A.B., 1996b. Stabilization of the Aravalli Craton of northwestern India at 2.5 Ga: an ion microprobe zircon study. *Chemical Geology* 12, 325–340.